5-2022

Geochemistry of Three Distinct Lewiston Quadrangle Pegmatites

ZaneAldeen Rahabi
Bates College, zrahabi@bates.edu

Geochemistry of Three Distinct Lewiston Quadrangle Pegmatites

A Senior Thesis

Presented to

The Faculty of the Department of Earth and Climate Sciences

Bates College

In partial fulfillment of the requirements for the

Degree of Bachelor of Science

By

ZaneAldeen Rahabi

Lewiston, Maine

April 22, 2022

Acknowledgements

I would first like to thank Eshita Samajpati for all of her help as the advisor of my senior thesis, which would not exist in its current state without her encouragement and support. Thank you to Phil Dostie for helping me crush, pulverize, powder, and polish my samples to prepare them for geochemical analysis—I couldn't have done it without you. Thank you to Amber Whittaker at the Maine Geological Survey for providing me with the inspiration for this thesis, as I would otherwise be entirely unaware of the existence of the three Lewiston Quadrangle pegmatite varieties. Thank you also to Dave West at Middlebury College for providing me with potential pegmatite sampling locations in the Bowdoinham Quadrangle, as my unfortunate inability to find them even with his assistance helped to shape my thesis into what it is today. A big thanks to Chris Halsted and everyone else at the Maine Geological Survey for helping me learn more about the geology of Maine, and for giving me the opportunity to study the geology of Mount David in greater detail, so that I could cite myself in my own thesis. Thank you to Alicia Cruz-Uribe at UMaine Orono for letting me analyze my quartz grains using the MAGIC lab, as half of my thesis would not exist without this vital data. Thank you to my mother, my father, and all of my friends for being so supportive of me throughout this entire process. Finally, thank you to all of my peers and professors in the Bates EACS department—both past and present—for making me feel at home here at Bates, for helping me acquire the skills and knowledge which I will surely need for future geology-related endeavors, and for being always appreciative of the cool rocks I've found on our many field trips together.

Table of Contents

Table of Figures

Table of Tables

Abstract

The Lewiston, Maine 15-minute Quadrangle is dominated by highly migmatized metasedimentary rocks, which are intruded by three apparently distinct pegmatite varieties, about which little is currently known. In order to classify these pegmatites according to several classification schemes, and to answer questions regarding their origins, the whole rock geochemistry of these pegmatites was analyzed through ICP-MS and ICP-OES, and their individual quartz grain geochemistry analyzed through LA-ICP-MS. The Muscovite + Tourmaline variety is found to be most similar to an LCT-leaning Mixed pegmatite, which likely crystallized at temperatures near 500 °C, and may have formed from either direct anatexis of the Sangerville Formation, or from residual granitic melts related to nearby granitoid units. The Garnet + Tourmaline variety is also found to be similar to an LCT-leaning Mixed pegmatite, which likely crystallized at a temperature similar to that of the Muscovite + Tourmaline variety, and may have potentially formed from the same source as that variety, after said source had become depleted in LREEs due to the first variety's formation. The Biotite variety is found to be most similar to an NYF-leaning Mixed pegmatite, which likely crystallized at higher temperatures near 600 °C, and likely formed from direct anatexis of the Vassalboro Formation. Geochemical evidence suggests that it is therefore accurate to classify all Lewiston Quadrangle pegmatites as entirely distinct pegmatite varieties.

1 Introduction

1.1 Pegmatites and Pegmatite Classification

Pegmatites are intrusive igneous rocks, often granitic in composition, and are characterized by an exceptionally coarse texture, with individual crystals averaging at least 2cm in diameter (Simmons and Webber 2008). While it was once widely believed that pegmatites formed as a result of very slow rates of cooling and crystal growth in intrusive magmas, currently-favored models suggest that pegmatites may instead form from either residual granitic melts, or as a direct product of partial melting during metamorphism, also called anatexis (Simmons and Webber 2008; Simmons et al. 2016; Webber et al. 2019; Müller et al. 2021). These melts tend to be enriched in incompatible components (such as rubidium or tantalum), volatiles (such as boron or fluorine), and rare earth elements, resulting in an increased diffusion rate, and a decreased crystallization temperature, nucleation rate, and viscosity—conditions which all strongly favor the formation of large crystals (Simmons and Webber 2008).

As pegmatites are characterized primarily by their large grain size, and tend to be enriched in incompatible and rare earth elements, their compositions may vary greatly. As a result, multiple schemes for their classification or division into separate categories have been proposed, mostly applicable to pegmatites of a granitic nature. The scheme established by Černý (1991) is the most widely-used today, which classifies pegmatites into three "petrogenetic families" based on their emplacement depth, metamorphic grade, and trace element signature: the LCT family (enriched in Lithium, Cesium, and Tantalum), the NYF family (enriched in Niobium, Yttrium, and Fluorine), and the Mixed family, which possesses characteristics typical of both the LCT and NYF families. This scheme was later revised by Černý and Ercit (2005) in order to also include pegmatites varieties which may not be as enriched in rare earth elements,

and to further subdivide the previous three petrogenetic families, resulting in a system featuring several classes, subclasses, types, and subtypes of pegmatites, differentiated by their depth, metamorphic grade, mineralogy, and geochemistry. All classes, subclasses, types, and subtypes can be found in Table 1.1. Another more recent scheme of pegmatite classification comes from Wise et al. (2021), where pegmatites are classified into six groups—differentiated by melt origin and geochemistry—with three groups derived from residual granitic melts, and the other three derived from anatexis. These six groups, along with their typical source rocks and geochemical signatures, can be found in Table 1.2.

THE CLASS SYSTEM OF GEOLOGICAL, PARAGENETIC AND GEOCHEMICAL CLASSIFICATION OF GRANITIC PEGMATITES

Class	Subclass	Type	Subtype
Abyssal (AB)	AB-HREE AB-LREE AB-U AB-BBe		
Muscovite (MS)			
Muscovite – Rare-element (MSREL)	MSREL-REE MSREL-Li		
Rare-element (REL)	REL-REE	allanite-monazite euxenite gadolinite	
	REL-Li	beryl	beryl-columbite beryl-columbite-phosphate
		complex	spodumene petalite lepidolite elbaite amblygonite
		albite-spodumene albite	
Miarolitic (MI)	MI-REE	topaz-beryl gadolinite-fergusonite	
	MI-Li	beryl-topaz MI-spodumene MI-petalite MI-lepidolite	

Table 1.1 Granitic pegmatite classes and associated subclasses, types, and subtypes. Adapted from Černý and Ercit (2005).

RMG (Residual melts of granite magmatism)			
Petrogenetic type - mineralogical group	RMG - Group 1	RMG - Group 2	RMG - Group 1+2
Typical source rock	S-type granites	A-type granites	I-type granites
Granite chemistry	Peraluminous	Peralkaline & metaluminous to mildly peraluminous	Peraluminous to metaluminous
Typical geochemical signatures	Be, Nb, Ta, P, Sn, Li, Cs	REE, Be, Nb, F	B, Be, REE, Nb, Ti, Li, Ca
DPA (Direct products of anatexis)			
Petrogenetic type - mineralogical group	DPA - Group 1	DPA - Group 2	DPA - Group 3
Typical source rock	Granulite to amphibolite facies metasediments and metaigneous rocks of granitic S-type	Granulite to amphibolite facies F-rich amphibolites and metaigneous rocks of granitic A-type signature	Granulite to amphibolite facies metagraywackes and metaigneous Al-rich
Typical geochemical signatures	Be, Nb, Ta, P, Li	REE, U, Be	Al, Be, B

Table 1.2 Pegmatite types, source rocks, and geochemical signatures from Wise et al. (2021).

1.2 Geology of Maine

The modern-day bedrock geology of Maine, as seen in Figure 1.1, is the result of a series of orogenic and metamorphic events primarily caused by the accretion of several exotic terrains onto the paleocontinent Laurentia due to tectonic processes in the ancient Iapetus Ocean. The Ordovician-aged Taconic Orogeny saw the passive margin of Laurentia collide with—and become subducted beneath—a complex volcanic island arc, resulting in a period of deformation, uplift, and igneous activity. This was followed by the Devonian-aged Acadian Orogeny, in which the microcontinent Avalonia was similarly accreted onto Laurentia, resulting in additional widespread deformation, metamorphism, and igneous activity affecting the majority of all Maine rocks. This particular orogeny was largely responsible for the formation of the Appalachian Mountains, which pass through modern-day Maine. Following this, the Late Devonian to Early Mississippian-aged Neo-Acadian orogeny resulted in tonalite-granitic magmatism, and up to granulite-facies metamorphism, with the intrusion of a large igneous pluton—the Sebago pluton—also occurring around this time in what is now southern Maine. The Late Pennsylvanian orogeny saw the formation of the Norumbega right-lateral fault system along the current Maine coastline, while the Permian-aged Alleghanian orogeny saw continued uplift and erosion of the Appalachian Mountains and further granitic intrusions, as the paleocontinent Gondwana collided

with Laurentia to form Pangaea (Marvinney 2012; Robinson et al. 1998, Bradley et al. 2016). The Mesozoic later saw the rifting of Pangaea and the opening of the Atlantic Ocean, resulting in widespread faulting and fracturing of Maine bedrock, and the intrusion of mafic dykes throughout southwestern and coastal Maine. Subsequent fracturing and faulting of Maine bedrock caused by and concurrent with Cenozoic uplift, erosion, glaciation, and post-glacial rebound is then responsible for the current bedrock geology of Maine as it can be seen today (Marvinney 2012). It is important to note that Maine as a whole is intruded by several pegmatitic bodies, considered by many to potentially result from igneous activity associated with the Neo-Acadian and Alleghanian orogenies, which may have resulted in the partial melting of those rocks affected by said orogenies (Simmons et al. 2016; Bradley et al. 2016, Marvinney 2012).

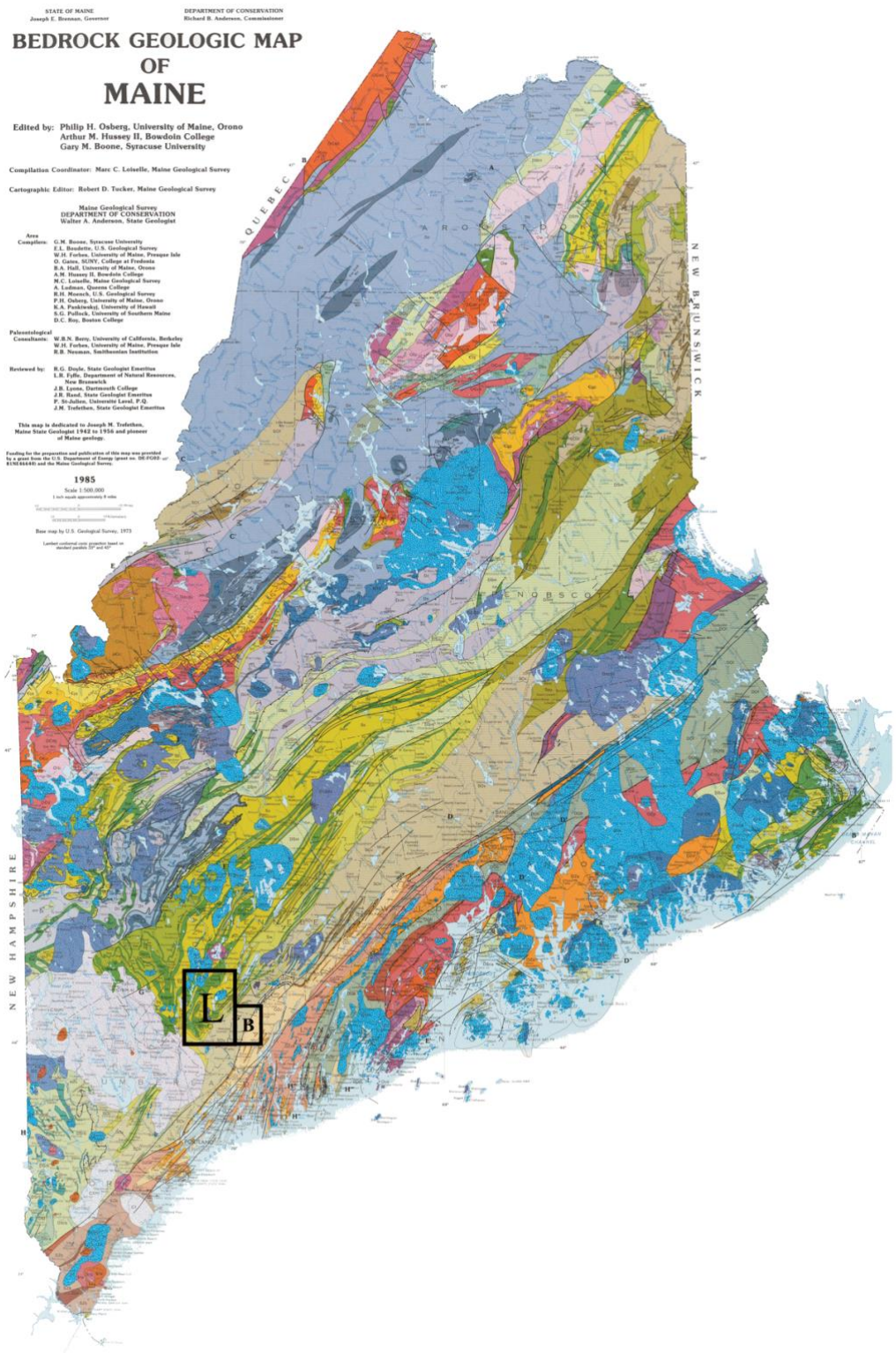

Figure 1.1 Bedrock map of Maine, adapted from Osberg et al. (1985). Locations of the Lewiston 15-minute Quadrangle (L) and the Bowdoinham 7.5-minute Quadrangle (B) are provided.

1.3 Regional Geology

The Lewiston Quadrangle falls within the southernmost portion of the shale-wacke sequence of south-central Maine, composed primarily of Silurian-aged wackes, shales, limestones, and conglomerates, which have been metamorphosed to granofels, schists, and marbles (Osberg 1988; Hussey 1983). Among the units which make up the shale-wacke sequence are the Waterville, Sangerville, Vassalboro, and Smalls Falls formations, which interfinger with one another over a large geographic area, and which are of particular interest to this study, as they are the primary metasedimentary units found within the Lewiston Quadrangle. Much like the majority of Maine, the region is overall multiply metamorphosed, ranging from a chlorite-grade zone in the north to a sillimanite-grade zone in the south (Osberg 1988).

The Waterville Formation consists of quartz-biotite-muscovite-sillimanite schist interbedded with quartz-plagioclase-biotite granofels and calc-silicate granofels, with occasional metalimestone and quartz-biotite-calcite granofels. The Sangerville Formation is quite complex, but is dominated by extensively-migmatized biotite-muscovite-quartz±sillimanite-garnet schist and quartz-plagioclase-biotite granofels. Subunits of the Sangerville Formation which are of particular interest to this study include an unnamed rusty-weathering sulfidic muscovite-biotite-sillimanite schist and garnet-rich biotite schist subunit, and the Patch Mountain subunit, which consists of interbedded calc-silicate granofels, quartzo-feldspathic biotite granofels, and marble (Hussey 1983). The Vassalboro Formation consists of quartz-plagioclase-biotite-hornblende granofels and schist interlayered with plagioclase-quartz-actinolite-diopside±biotite granofels (Hussey 1983; West and Cubley 2010). Finally, the Smalls Falls Formation consists of rusty-weathering sillimanite schist and quartz-plagioclase-biotite granofels (Hussey 1983).

The region shows evidence of three sets of folds, and is thought to have been affected by three major metamorphic events. The exact mechanisms responsible for the formation of the

oldest set of folds is currently unknown, as evidence for these F_1 folds is mostly indirect. However, the first major metamorphic event known to have affected this region is approximately coeval with F_2 folds, while the second event is coeval with F_3 folds. It is this event—assigned a Late Devonian age—which is thought to be responsible for most of the observed metamorphic features. A third, possibly Carboniferous-aged metamorphic event is thought to exist based on the presence of chlorite pseudomorphs after cordierite and biotite in some shale-wacke sequence rocks. Juxtaposed stratigraphy suggests that a large thrust fault, the Messalonskee Lake thrust, passes through this region and predates F_2 folding. This thrust fault is thought to dip to the east, suggesting transport to the west, and places older formations such as the Waterville and Vassalboro formations above the younger Sangerville Formation (Osberg 1988).

1.4 Study Area

The bedrock geology of the Lewiston, Maine 15-minute Quadrangle was mapped most recently by Hussey (1983), who found that it is primarily dominated by the aforementioned Silurian-aged metasedimentary rocks of the Sangerville, Waterville, Small Falls, and Vassalboro formations, which have been heavily migmatized due to intense heat during high-grade metamorphism. These metasedimentary rocks are intruded by granite, granodiorite, and pegmatite units, all of which were originally assigned to the Early Devonian-aged New Hampshire Plutonic Series, but are likely much younger in age, as nearby Maine pegmatites and granites range from Late Devonian (West and Cubley 2010) to Permian (Bradley et al. 2016; Simmons et al. 2016) in age. Many mafic dykes can be found throughout the Lewiston Quadrangle as well, and though radiometric dating does not yet exist for these dykes, they likely correlate with Jurassic and Triassic igneous activity associated with the rifting of Pangaea (Hussey 1983). The aforementioned Messalonskee Lake thrust is noted to pass through the

Lewiston Quadrangle as well, placing the older Vassalboro Formation above the younger Sangerville Formation (Osberg 1988; Whittaker, personal communication). A colorized version of the Hussey (1983) map can be seen in Figure 1.2.

Viewing this map, it is important to note that although the Lewiston Quadrangle granite and granodiorite units were mapped in 1983, the pegmatite bodies unfortunately were not. Researchers from Middlebury College and the Maine Geological Survey who are currently re-mapping the quadrangle to a more detailed degree have reported three distinct varieties of pegmatite which exist within its bounds. All varieties primarily consist of quartz and feldspar, but otherwise differ in mineral assemblage: the first variety contains garnet and tourmaline, the second contains muscovite and tourmaline, and the third contains only biotite. Notably, the only tourmaline variety found in the Lewiston Quadrangle pegmatites is of the schorl variety (Whittaker, personal communication). This analysis of the Lewiston Quadrangle pegmatites is at odds with that of Hussey (1983), where it is implied that all Lewiston Quadrangle pegmatites share the same mineral assemblage, consisting of quartz, albite, microcline, biotite, muscovite, garnet and schorl. In either case, the Lewiston Quadrangle pegmatites would be referred to as "simple pegmatites", as they contain few exotic minerals (Stemprok 1989). It should be noted that a pegmatite distribution similar to the one reported by Whittaker is also noted to occur in the adjacent Bowdoinham 7.5-minute Quadrangle, which contains a distinct muscovite-rich variety, tourmaline-rich variety, and biotite-rich variety, with the latter two occurring in close proximity within the same rock unit (West and Cubley 2010).

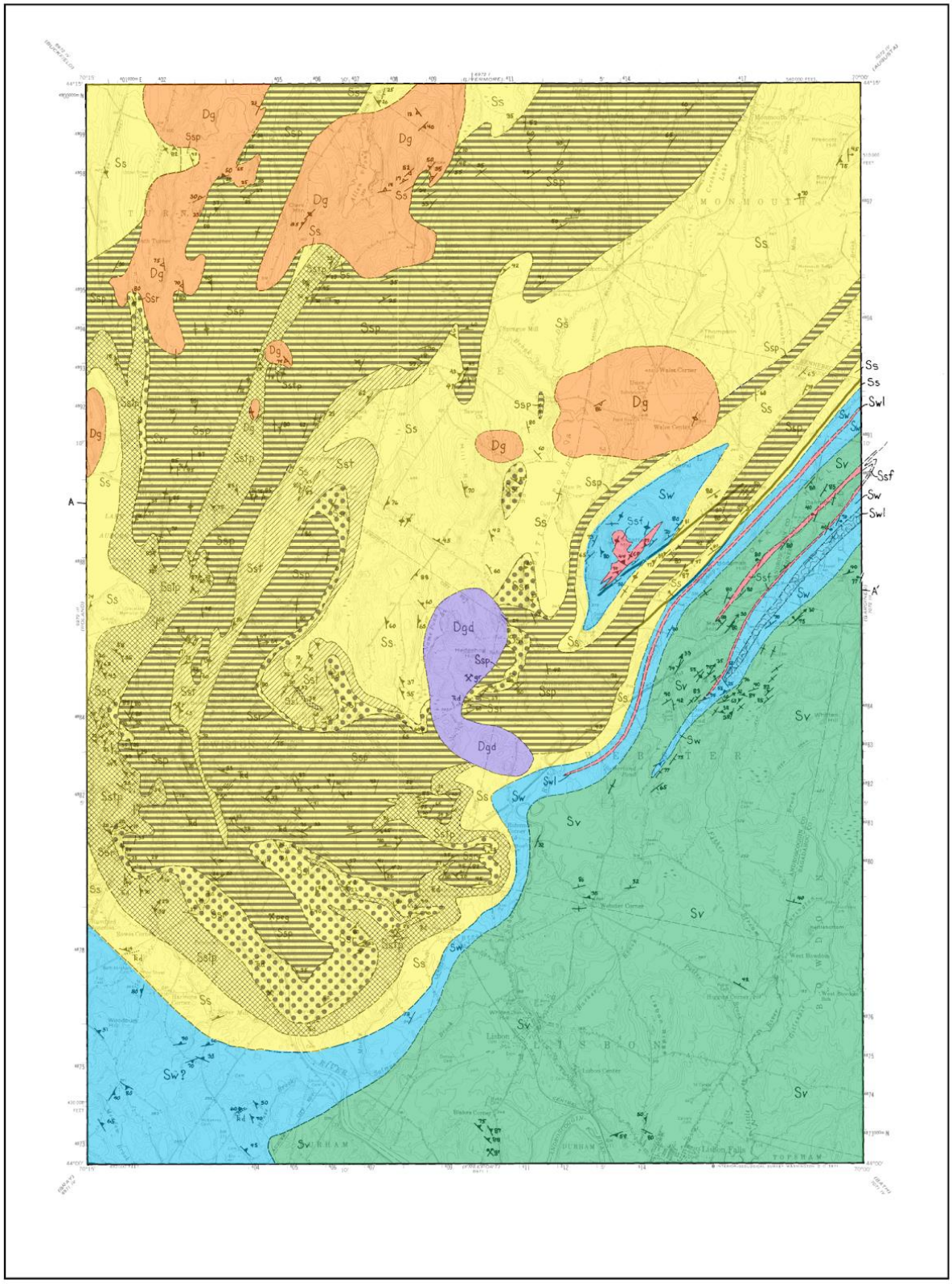

Figure 1.2 Bedrock map of the Lewiston 15-minute Quadrangle, adapted from Hussey (1983).

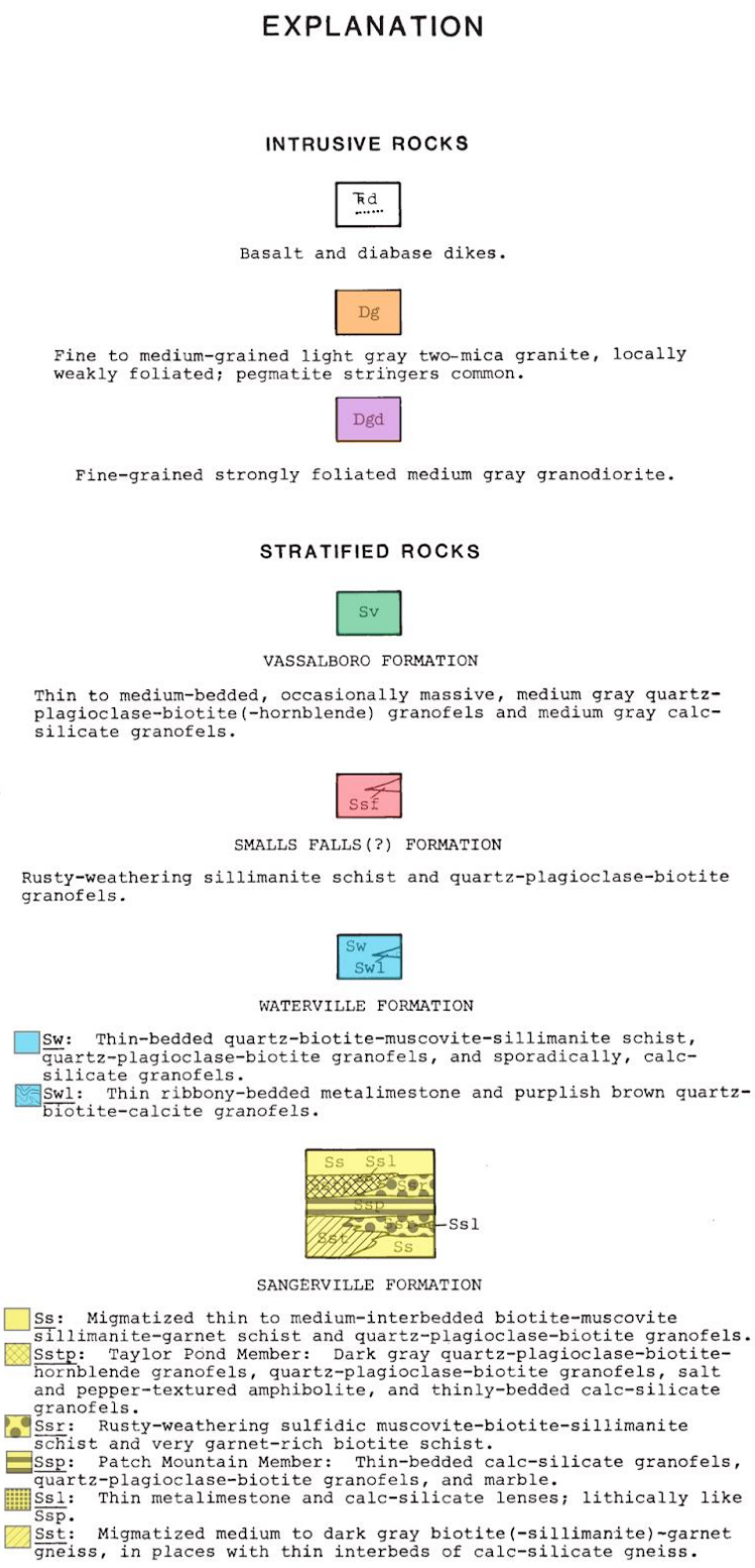

Figure 1.3 Lewiston 15-minute Quadrangle map legend, also adapted from Hussey (1983).

1.5 Objectives

Little information currently exists regarding the Lewiston Quadrangle pegmatites. It is intriguing that several different distinct varieties of pegmatite exist concurrently and in such close proximity within the Lewiston Quadrangle and adjacent quadrangles, sometimes even within the same host rock unit. It is currently unknown whether these pegmatites formed from residual granitic melt or due to direct anatexis of the surrounding metasedimentary rocks, and it has yet to be proven whether these are truly three distinct varieties of pegmatite, or simply the same pegmatite with different minerals concentrated in specific areas. These pegmatites also have yet to be formally classified according to any of the previously-mentioned pegmatite classification schemes. This study aims to use geochemical whole rock and individual quartz grain analysis in order to answer questions regarding the origins of these three apparently distinct Lewiston Quadrangle pegmatite varieties. Such information could be of import towards the current endeavor to map the Lewiston Quadrangle, and could provide additional insights into the nature of simple pegmatites, which are underrepresented in the field of pegmatite research.

2 Methods

2.1 Location Scouting & Sampling

As pegmatite locations were not mapped in great detail in 1983, and any local differences in pegmatite composition were not yet considered evidence of distinct pegmatite varieties (Hussey 1983), sampling locations for each pegmatite variety were determined through a combination of field observations and personal communications with current Lewiston Quadrangle researchers. Mount David, a small hill near Bates College, was provided as one locality for the Garnet + Tourmaline (GT+T) variety (Whittaker, personal communication; Rahabi, 2021), however sampling at this location was deemed infeasible due to the site's heritage and adjacency to residences. Field observations of known pegmatite outcrops in Lewiston revealed Lewiston City Quarry as another locality for the GT+T pegmatite variety, and it was from this site that samples were taken. At the advice of current Lewiston Quadrangle researchers, samples of the Muscovite + Tourmaline (MS+T) pegmatite variety were taken from a road cut adjacent to the Maine Turnpike Exit 80 northbound onramp in Lewiston, and samples of the Biotite (BT) variety were taken from an easily-accessible outcrop located on W Burrough Rd in the nearby town of Bowdoinham (Whittaker, personal communication). Samples were obtained using an Estwing rock hammer, and were taken from multiple different points at each outcrop, in order to hopefully represent a more generalized example of each pegmatite variety. Sampling locations are marked on the satellite map seen in Figure 2.1.

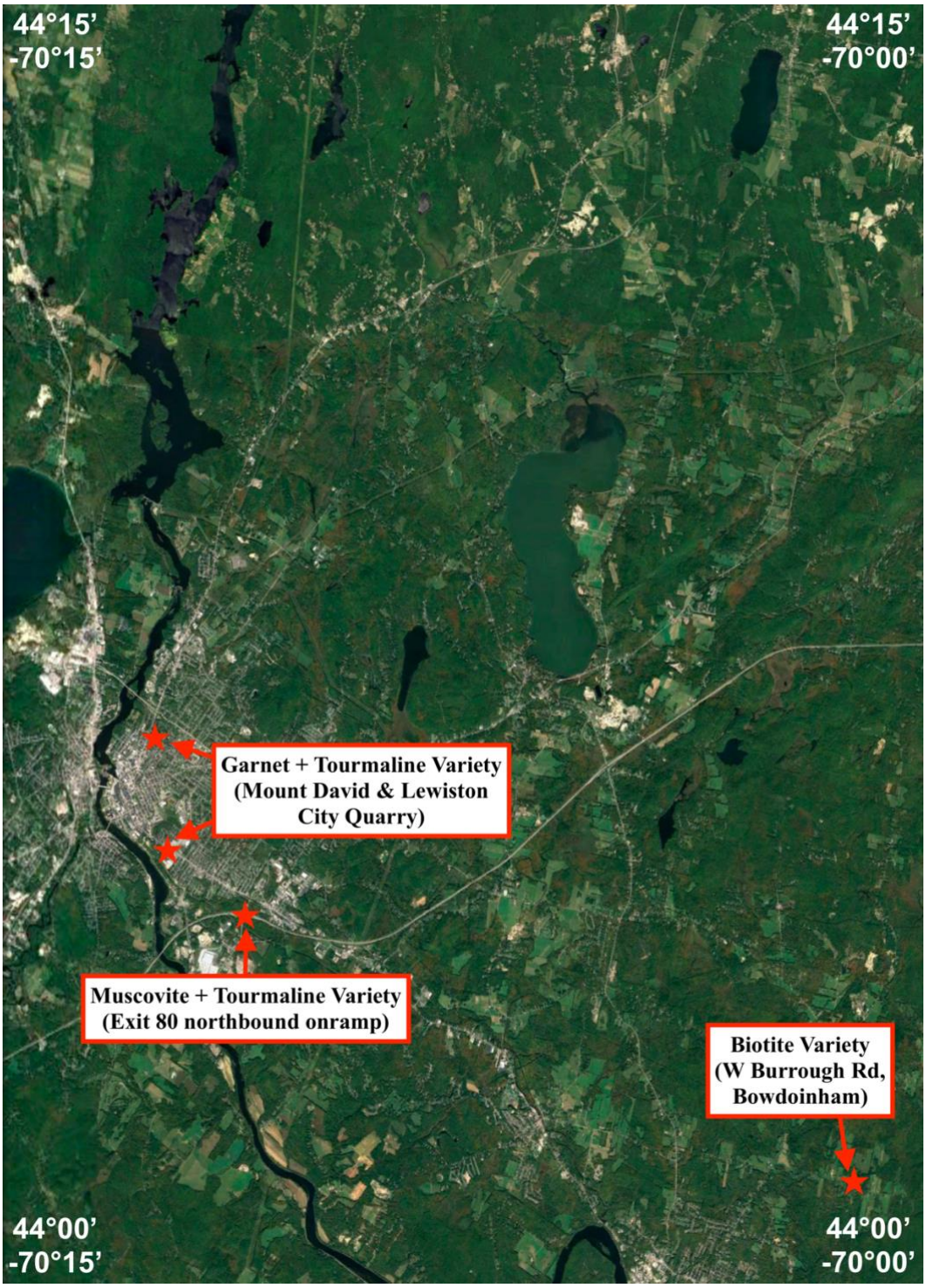

Figure 2.1 Satellite map of the Lewiston 15-minute quadrangle, with sampling locations for each pegmatite variety shown. No samples were taken from Mount David, though it is a known locality for the Garnet + Tourmaline Variety.

2.2 Sample Preparation

In order to prepare the pegmatites for geochemical whole rock analysis, samples were first reduced to a manageable size using a sledgehammer, then fed into a Braun Chipmunk rock crusher (Figure 2.2a, right) and crushed into a "pegmatite gravel" with a grain size of approximately 5mm. This material was homogenized, and then further refined using a Bico, Inc. rock pulverizer (Figure 2.2a, left), reducing it to a "pegmatite sand" with a grain size of approximately 1mm. The pegmatite sand was again homogenized by hand mixing, and a portion of this sand was placed into a Spex Industries, Inc. mixer/mill (Figure 2.2b) for 5 minutes in order to reduce it to a fine powder suitable for geochemical analysis. This pegmatite powder was then homogenized one more time before being sent off for analysis. This process was performed individually for samples of each pegmatite variety, so that the end result was three rock powders, each representative of a different pegmatite variety found in the Lewiston Quadrangle.

From the remaining pegmatite sand, nine grains of quartz were carefully removed using tweezers—three from each pegmatite variety—and set in epoxy resin in order to create grain mounts. These grain mounts were then polished using 600 grit sandpaper on an Ecomet 3 variable speed grinder-polisher (Figure 2.2c) in order to reveal the surface of the quartz grains. This resulted in three grain mounts, each one containing three quartz grains from a different pegmatite variety. Three grains were chosen from each variety in order to check the quality and consistency of the data acquired.

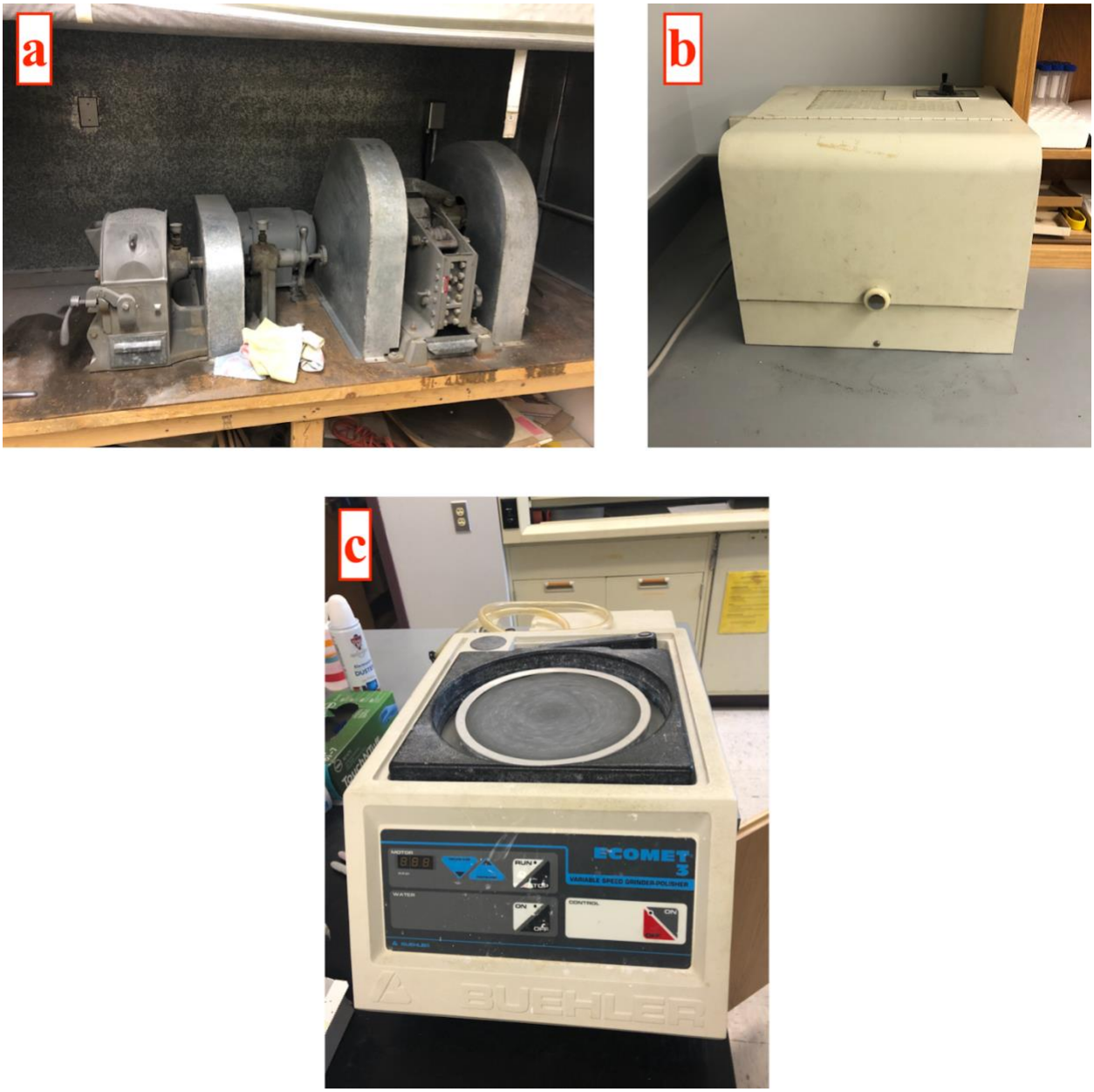

Figure 2.2 a) Braun Chipmunk rock crusher (right) and Bico, Inc. rock pulverizer (left). b) Spex Industries, Inc. mixer/mill. c) Ecomet 3 variable speed grinder-polisher with 600 grit sandpaper.

2.3 Analytical Methods

Whole rock analysis of the pegmatite samples for major and trace elements—including rare earth elements—was performed by Actlabs, and was achieved using inductively coupled plasma mass spectrometry (ICP-MS) and inductively coupled plasma optical emission

spectrometry (ICP-OES). ICP-OES was used to determine major oxide concentrations, while ICP-MS was used to determine trace element concentrations. ICP-MS was deemed more suitable for the collection of trace elements than ICP-OES due to its lower detection limit, able to detect concentrations in the range of 1-10 parts per trillion (ppt), whereas ICP-OES has a limit of only 1-10 parts per billion (ppb) (Tyler 1995).

These methods of determining element concentration work similarly up until a certain point. For both methods, a solid sample is digested into a liquid solution, and this liquid is nebulized and subsequently atomized and ionized by argon plasma, which has been heated by induction. In the case of ICP-MS, the ions are then focused into an ion beam, which is guided into a quadrupole mass analyzer in which ions are separated according to their mass-charge ratio. These ions are counted by a detector, allowing the concentration of ions of a specific mass-charge ratio to be determined for the sample (Wilschefski and Baxter 2019). A diagram of how this process works can be found in Figure 2.3. ICP-OES functions slightly differently post-ionization: the atoms and ions of the sample become excited by the thermic energy of the plasma, causing their electrons to move into higher energy states. When the electrons subsequently move back down from their excited states, the excess energy is released as light. This light falls onto a prism, which separates it into a spectrum of individual wavelengths that are characteristic for that specific atom or ion. A computer then analyzes these spectra in order to determine the concentration of that atom or ion in the sample (Sharma 2020).

The mounted quartz grains were analyzed using laser ablation inductively coupled plasma mass spectrometry (LA-ICP-MS) at the University of Maine's MicroAnalytical Geochemistry and Isotope Characterization Laboratory in order to determine their concentrations of lithium, beryllium, boron, aluminum, titanium, germanium, and rubidium (Woodhead et al.

2007). LA-ICP-MS functions similarly to ICP-MS, but rather than digesting solid samples into a liquid solution which is then aerosolized, a small portion of the solid sample is instead directly vaporized using a high-powered laser beam, improving atomization and resulting in less contamination of the sample (Miliszkiewicz et al 2015). Post-vaporization, the process is the same as it would be for traditional ICP-MS. A line of 10 spots was analyzed across each grain with inclusions and spikes filtered out. NIST-612 was used as the primary reference material, with ^{28}Si as the internal standard element. Trace element mass fractions were determined using the Trace Elements DRS in iolite4 (Paton et al. 2011). NIST-610 and spots on the Bishop Tuff quartz were run as secondary reference materials. Analysis parameters were a 100 μm spot, with a repetition rate of 10 Hz and a beam energy fluence of 3.6 J/cm^2. Reference materials were run in blocks of 2 before and after every 30 unknowns. Each analysis consisted of 10sec of laser warmup during background collection, 30sec of ablation, and 10sec of washout.

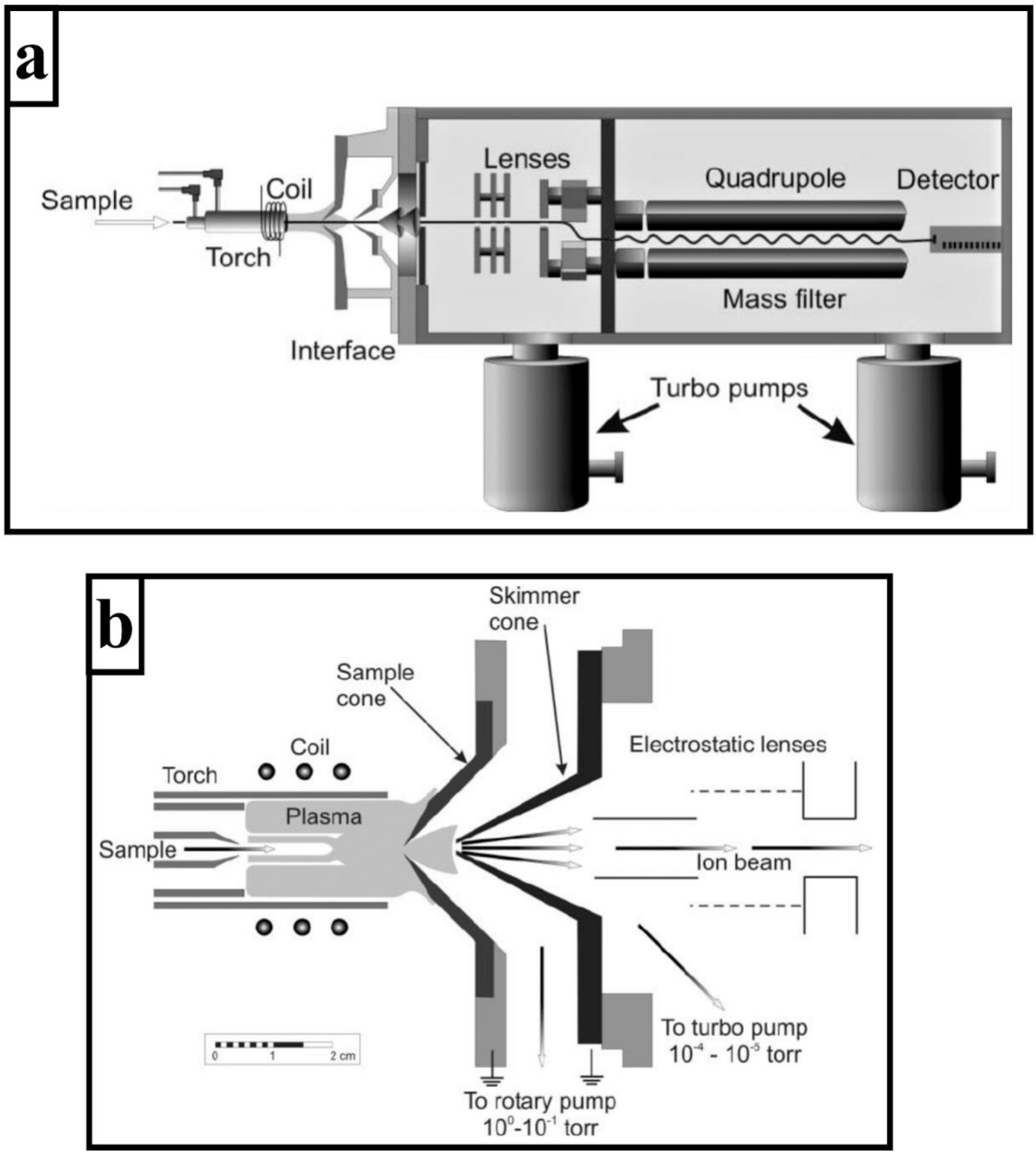

Figure 2.3 a) Diagram of the inner mechanism of an ICP-MS system. b) Close-up of mechanisms used for sample atomization, ionization, and ion beam focusing. Both diagrams adapted from Wilschefski and Baxter (2019).

3 Results

3.1 Whole Rock Major Oxides

The major oxide data for each pegmatite variety is quite similar, with a few minor differences. All pegmatites contain >70 wt% SiO_2, >10 wt% Al_2O_3, and >1 wt% Fe_2O_3, Na_2O, and K_2O. All other oxides are below 1 wt%. The BT variety contains the most SiO_2, MgO, and TiO_2 of any variety, and the least Na_2O. The MS+T variety contains the most Al_2O_3, K_2O, and of any variety, and the least SiO_2, Fe_2O_3, MgO, CaO, and TiO_2. The GT+T variety contains the most Fe_2O_3, CaO, and Na_2O of any variety, and the least K_2O. Exact values for these oxides can be found in Table 3.1. Figure 3.1 shows the three pegmatites plotted on a total alkali-silica (TAS) diagram, and reveals that the MS+T pegmatite variety is the only variety which falls within the alkali granite range, with the BT and GT+T varieties falling outside the granite or alkali granite range due to their higher silica content and lower overall alkali content. Figure 3.2 shows the three pegmatite varieties plotted on an A/CNK-A/NK plot, revealing that all pegmatite varieties are peraluminous in nature.

Table 3.1 Major oxides for all three pegmatite varieties (wt%).

Oxide	SiO_2	Al_2O_3	Fe_2O_3	MnO	MgO	CaO	Na_2O	K_2O	TiO_2	P_2O_5	LOI	Total
Detection Limit	0.01	0.01	0.01	0.001	0.01	0.01	0.01	0.01	0.001	0.01		0.01
BT peg	77.2	11.22	1.92	0.021	0.22	0.92	2.64	4.28	0.187	0.05	0.39	99.05
MS+T peg	72.26	15.38	1.11	0.048	0.09	0.37	3.34	5.47	0.029	0.09	0.77	98.96
GT+T peg	74.79	15.13	2.16	0.282	0.14	0.95	5.57	1.11	0.03	0.08	0.18	100.4

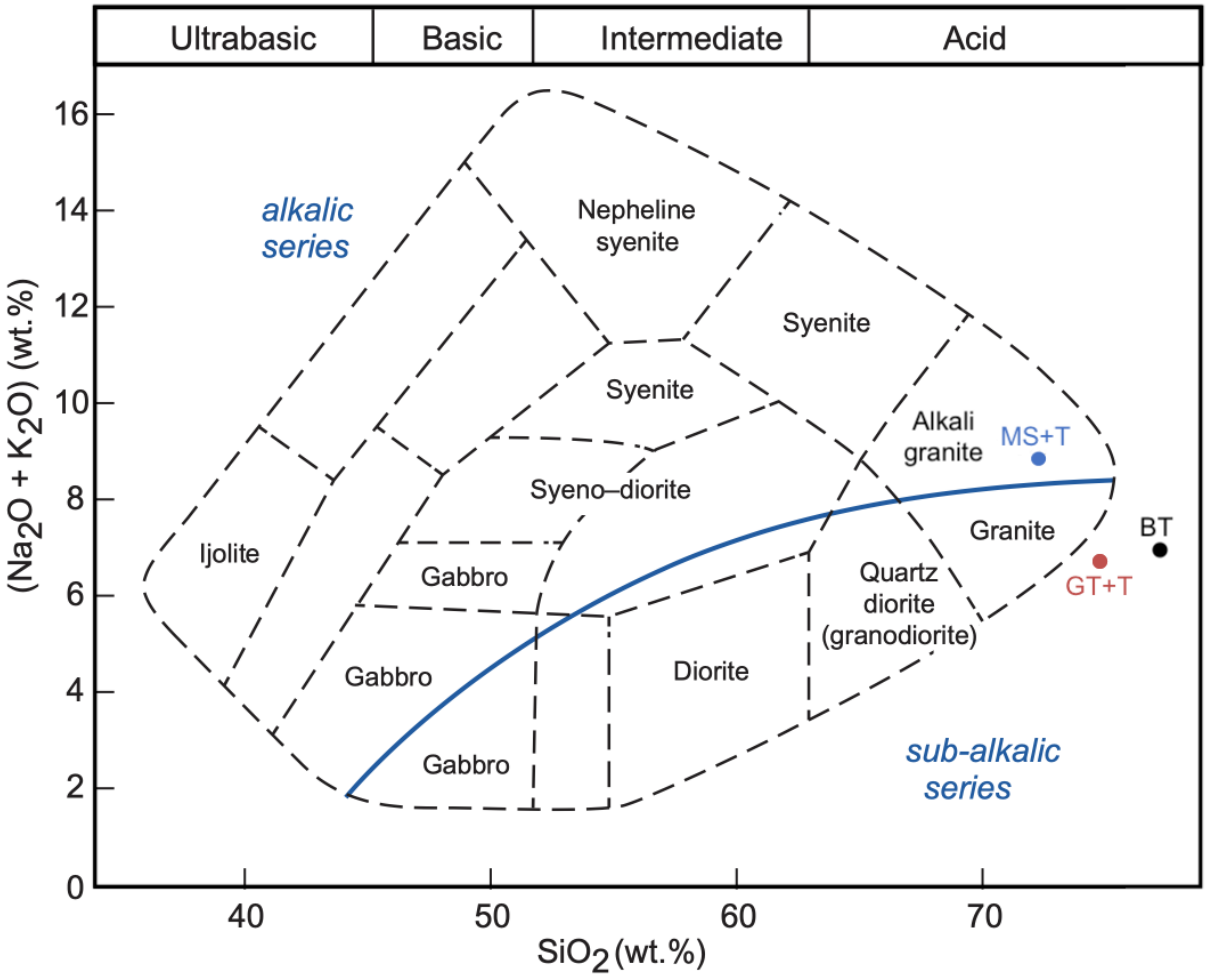

Figure 3.1 TAS diagram for plutonic rocks with all three Lewiston Quadrangle pegmatite varieties plotted. The blue line serves to differentiate the alkalic series from the sub-alkalic series. Adapted from Rollinson and Pease (2021).

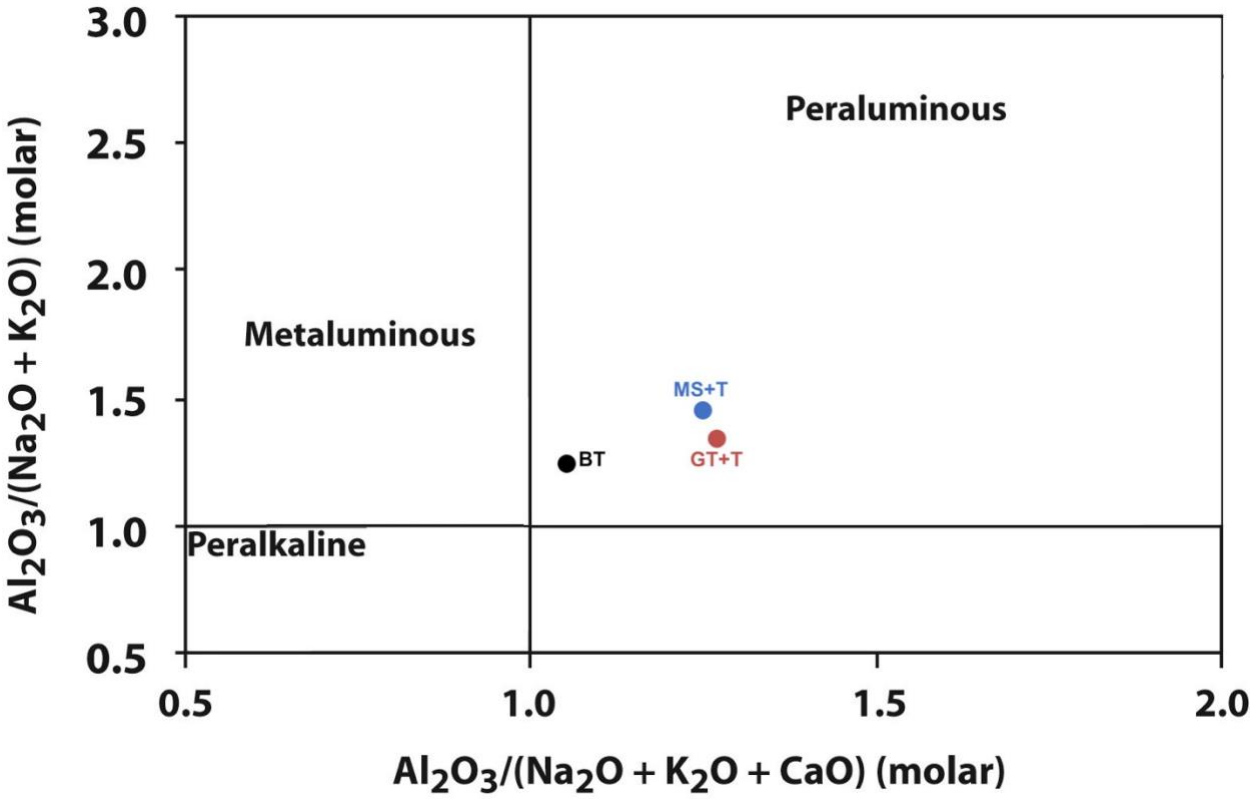

Figure 3.2 A/CNK-A/NK plot with all three Lewiston Quadrangle pegmatite varieties plotted, adapted from Mbowou et al. (2015).

3.2 Whole Rock Trace Elements

CI chondrite-normalized spidergram and rare earth element (REE) plots show notable differences between each pegmatite variety. General trends seen in Figure 3.3 show that all pegmatite varieties are notably depleted in Ba, Sr, Eu, and Ti, and notably enriched in Rb, Th, U, and Ta. Figure 3.4 shows that the BT variety exhibits a strongly negative Eu anomaly, while Eu concentrations for the GT+T and MS+T varieties were below the analytical detection limit, as seen in Table 3.2. Elements of particular relevance to this study include Cs, Nb, Ta, Y, and REEs. Figure 3.3 shows that all pegmatite varieties are depleted in Nb in comparison to Ta. Cs enrichment is unremarkable in all three pegmatite varieties, but GT+T is notably the only variety in which Cs is more enriched than the adjacent Rb. GT+T also appears enriched in Y, while

other varieties are comparatively depleted. Figure 3.4 shows that the BT and MS+T varieties are more enriched in light rare earth elements (LREEs) compared to heavy rare earth elements (HREEs), while the GT+T variety is more enriched in HREEs in comparison to LREEs.

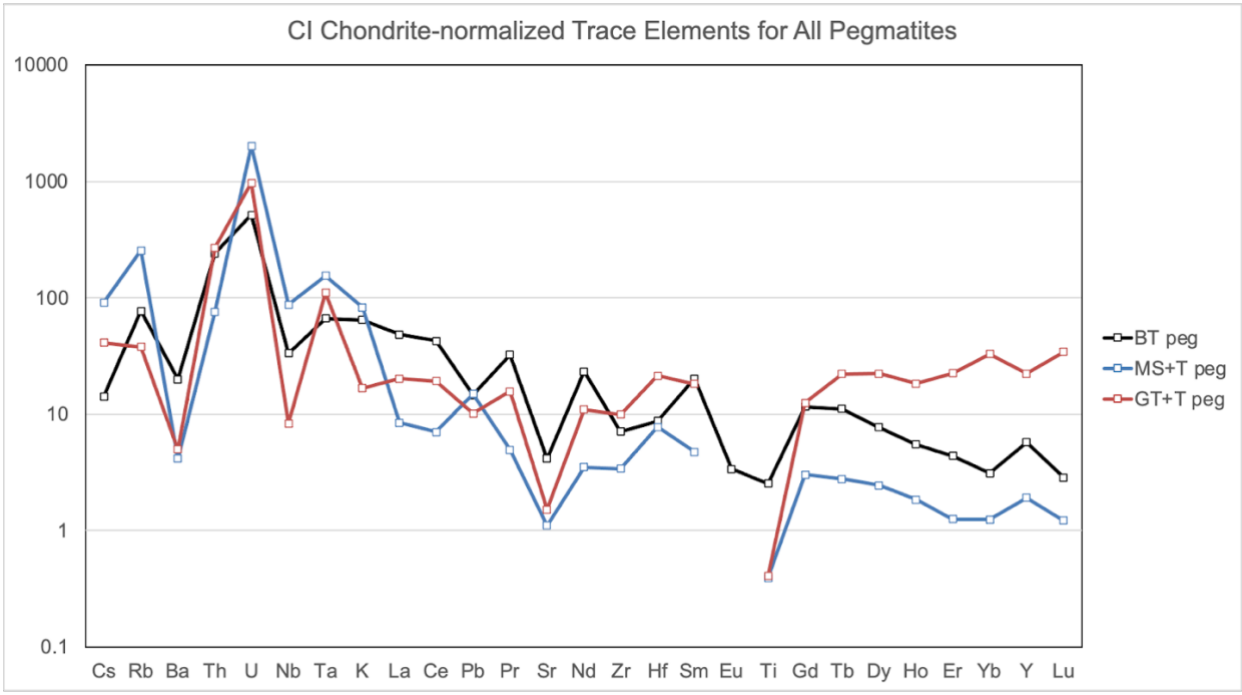

Figure 3.3 CI chondrite-normalized plot of trace elements from whole rock analysis of each of the three pegmatite varieties, including rare earth elements, K, and Ti. Normalized to chondrite values from McDonough and Sun (1995).

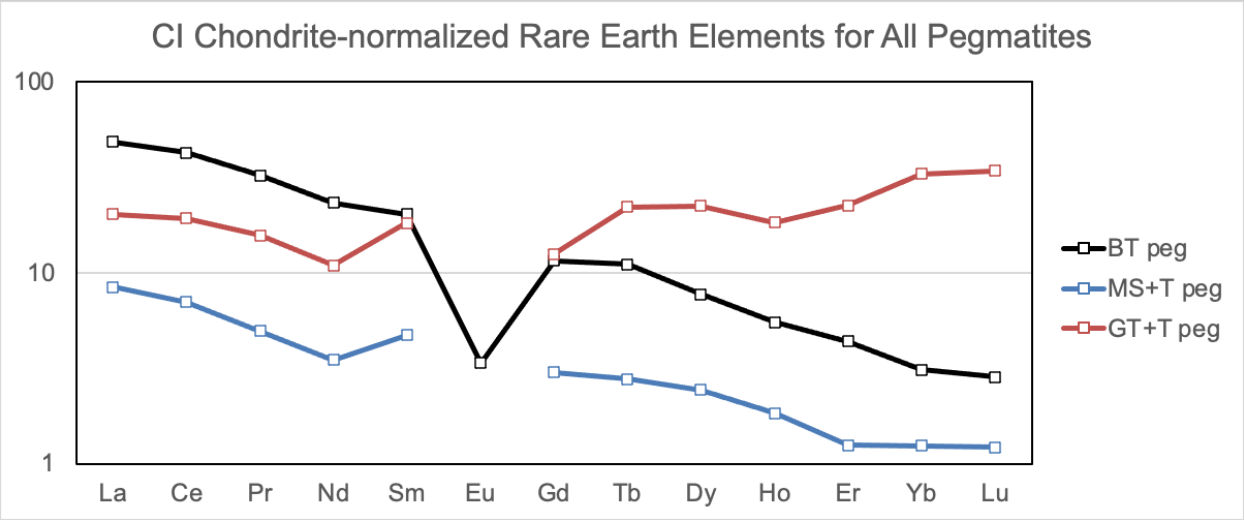

Figure 3.4 CI chondrite-normalized plot of rare earth elements for each variety. Normalized to chondrite values from McDonough and Sun (1995).

Table 3.2 Trace elements for all three pegmatite varieties (ppm)

Element	Sc	Be	V	Ba	Sr	Y	Zr	Cr	Co	Ni	Cu	Zn	Ga	Ge	As
Detection Limit	1	1	5	2	2	1	2	20	1	20	10	30	1	1	5
BT peg	3	2	6	48	30	9	27	< 20	4	< 20	< 10	40	19	1	< 5
MS+T peg	2	9	< 5	10	8	3	13	< 20	2	< 20	< 10	50	36	2	< 5
GT+T peg	4	8	< 5	12	11	35	38	< 20	6	< 20	< 10	70	26	2	81

Element	Rb	Nb	Mo	Ag	In	Sn	Sb	Cs	La	Ce	Pr	Nd	Sm	Eu	Gd
Detection Limit	2	1	2	0.5	0.2	1	0.5	0.5	0.1	0.1	0.05	0.1	0.1	0.05	0.1
BT peg	177	8	< 2	< 0.5	< 0.2	2	< 0.5	2.7	11.5	26.1	3.01	10.6	3	0.19	2.3
MS+T peg	584	21	< 2	< 0.5	< 0.2	25	< 0.5	17.3	2	4.3	0.46	1.6	0.7	< 0.05	0.6
GT+T peg	87	2	< 2	< 0.5	< 0.2	7	< 0.5	7.8	4.8	11.8	1.46	5	2.7	< 0.05	2.5

Element	Tb	Dy	Ho	Er	Tm	Yb	Lu	Hf	Ta	W	Tl	Pb	Bi	Th	U
Detection Limit	0.1	0.1	0.1	0.1	0.05	0.1	0.01	0.2	0.1	1	0.1	5	0.4	0.1	0.1
BT peg	0.4	1.9	0.3	0.7	0.08	0.5	0.07	0.9	0.9	43	0.7	36	5.2	7	3.8
MS+T peg	0.1	0.6	< 0.1	0.2	< 0.05	0.2	0.03	0.8	2.1	26	2.9	37	0.6	2.2	14.9
GT+T peg	0.8	5.5	1	3.6	0.73	5.3	0.84	2.2	1.5	64	0.9	25	< 0.4	7.8	7.2

3.3 Quartz Analysis

General trends seen in Figure 3.5 show that quartz grains taken from the BT pegmatite variety generally have the lowest concentrations of all selected elements except in the case of Ti. It is difficult to determine whether GT+T or MS+T quartz has the lowest concentrations of Ti, but BT quartz has by far the highest concentrations of that element. MS+T quartz has the greatest concentrations of Al, Ge, and Li, while GT+T quartz has the greatest concentrations of B. While BT quartz contains the lowest concentrations of Be, it is debatable whether GT+T or MS+T quartz has the highest concentrations, due to the presence of a large low-concentration outlier within one of the grains of GT+T quartz. Disregarding this outlier, GT+T and MS+T quartz grains generally have notably similar concentrations of Ti, B, and Be. While testing was performed in order to determine Rb concentrations for all quartz grains in addition to the elements seen here, Rb concentrations were unfortunately below the detection limit for all grains analyzed and therefore could not be recorded.

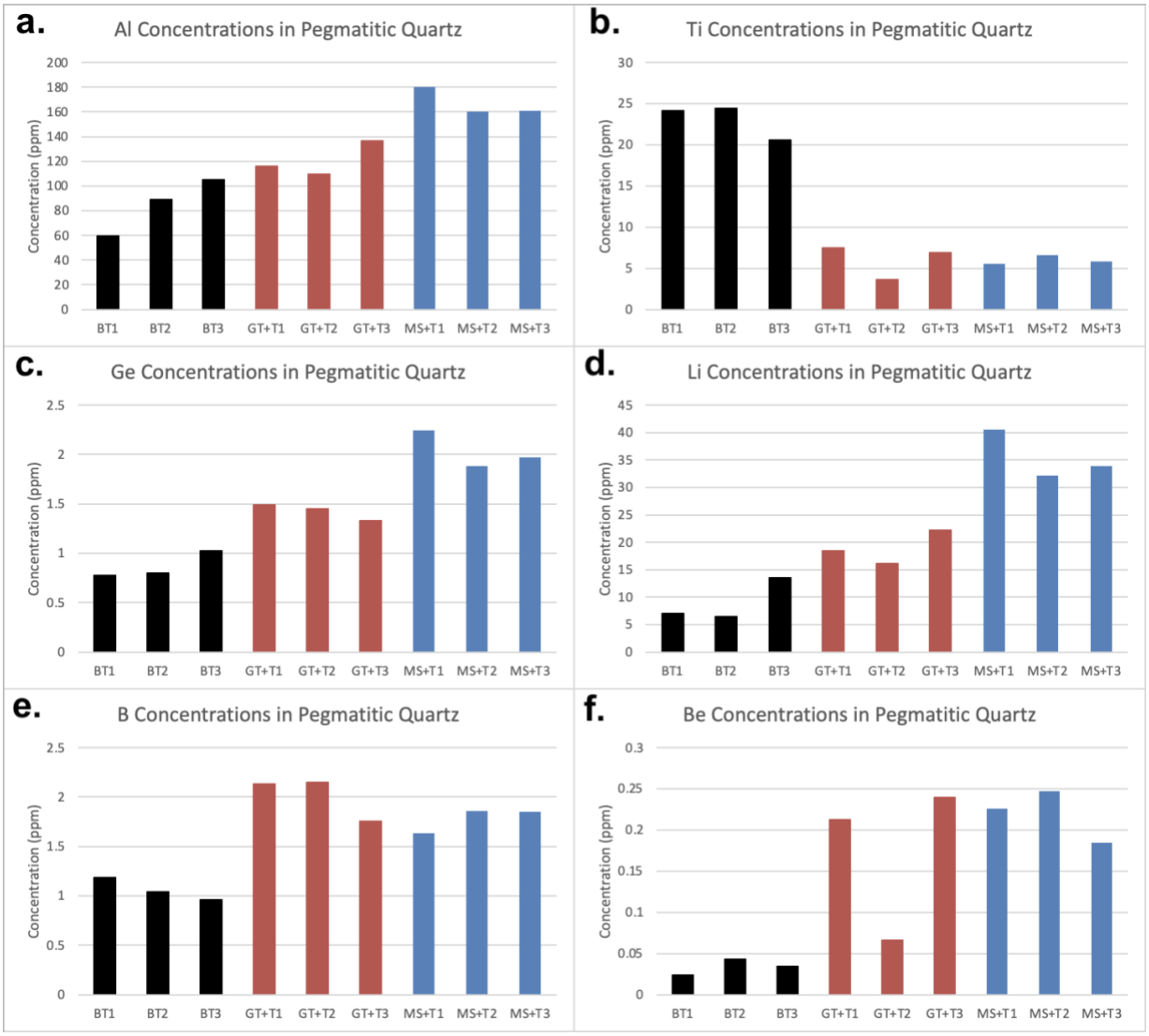

Figure 3.5 Concentrations of selected elements in quartz grains from each pegmatite variety.

Table 3.3 Concentrations of selected elements in pegmatitic quartz grains (ppm)

Element:		Al	Ti	Ge	Li	B	Be
BT peg quartz grains	BT1	59.70067	24.17426	0.776543	7.040677	1.185826	0.023732
	BT2	88.93094	24.40202	0.803136	6.456688	1.041944	0.042524
	BT3	104.93	20.5736	1.028014	13.57983	0.960854	0.034647
GT+T peg quartz grains	GT+T1	115.9301	7.485358	1.48642	18.4474	2.135735	0.212675
	GT+T2	109.2901	3.645798	1.445891	16.09807	2.151763	0.065748
	GT+T3	136.5564	6.929493	1.327308	22.21722	1.754656	0.239199
MS+T peg quartz grains	MS+T1	180.0355	5.585972	2.243892	40.6147	1.635125	0.225788
	MS+T2	160.0852	6.630734	1.885949	32.13419	1.856988	0.246775
	MS+T3	160.9636	5.854501	1.974401	33.86004	1.849512	0.184873

4 Discussion

4.1 Mineralogy and Texture

As previously mentioned, the three pegmatite varieties found throughout the Lewiston Quadrangle have noticeably different mineral assemblages and textures, which could provide some insights into their origins. The BT pegmatite variety features a noticeably smaller grain size than either of the other two varieties found within the quadrangle, appearing more similar to a granite at times than a pegmatite, which suggests that it may have undergone a cooling process very different from that of either other variety. While all pegmatite varieties contain quartz and feldspar, this variety contains only biotite in addition to these minerals, apparently containing no tourmaline nor muscovite, and only very rarely containing garnet. Contrastingly, the MS+T variety exhibits the usual large grain size indicative of a pegmatite, and apparently contains no biotite or garnet, instead containing only black tourmaline and muscovite along with the usual quartz and feldspar. Some areas of the MS+T variety contain no tourmaline at all, such as a portion of the Exit 80 outcrop which runs alongside Alfred A. Plourde Parkway, suggesting that pegmatite composition may vary greatly even within a single outcrop. Finally, the GT+T variety contains abundant garnet and black tourmaline, and exhibits a grain size similar to that of the MS+T variety. During sampling, muscovite was found to exist within the GT+T pegmatite at the Lewiston City Quarry in association with basaltic dikes, likely formed as a result of contact metamorphism. Muscovite was also found to exist within the GT+T pegmatite on the summit of Mount David, but only within a very small zone, which has been interpreted as a crystallization front where the very last, highly fractionated portions of the GT+T melt at this site pooled before finally crystallizing (Rahabi 2021). Interestingly enough, this muscovite-rich zone contains little garnet, perhaps implying a relationship rooted in fractionation between the MS+T and GT+T pegmatite varieties. Sillimanite and biotite were also noted to be found on the summit of Mount

David, though these minerals were determined to be xenoliths from the surrounding Sangerville Formation, and not a part of the pegmatite itself (Rahabi 2021).

4.2 Geochemistry

4.2.1 Whole Rock Geochemistry

As seen in Figure 3.3, all three pegmatite varieties are enriched in highly incompatible elements such as U, Th, and Ta, reflective of their origins as an incompatible-rich melt derived from either residual granitic melt, or anatexis during metamorphism (Simmons and Webber 2008). All varieties are also greatly depleted in Ba, Sr, and Eu relative to other trace elements, implying that plagioclase—a mineral into which these elements are preferentially incorporated (Fedele et al. 2015)—may have crystallized out of the pegmatitic melt early during the early stages of cooling. As all varieties are also greatly depleted in Ti, it is likely that Ti oxides may have fractionated out from the melts at some point during their solidification. Figure 3.4 shows that the GT+T variety is noticeably highly enriched in HREEs—more so than any other variety—likely due to this pegmatite being the only variety which contains large amounts of garnet, into which HREEs are preferentially incorporated (White 2013). This results in the positive REE slope displayed by the GT+T variety, whereas the other two varieties exhibit negative slopes. The negative slope displayed by the other two varieties is again reflective of those pegmatites' relative enrichment in incompatible elements, as LREEs are traditionally considered highly incompatible (Miller 1982, White 2013). La/Lu ratios for each variety based on the chondrite-normalized values seen in Figure 3.4 are 0.59 for the GT+T variety, 17.05 for the BT variety, and 6.92 for the MS+T variety. Based on these ratios, one can assume that the MS+T and BT+T varieties derive from enriched sources, while the GT+T pegmatite is the only variety with an La/Lu ratio of less than 1, implying that it derives from a depleted source.

4.2.1 Pegmatitic Quartz Geochemistry

The geochemistry of pegmatitic quartz may be used to distinguish pegmatites of different classifications, as established by Müller et al. (2021). Figures 4.1 and 4.2 show quartz grains from the three Lewiston Quadrangle pegmatite varieties plotted on binary trace element plots adapted from Müller et al. (2021), which also display data for pegmatitic quartz grains from elsewhere in the world, with their classifications according to both Černý (1991) and Wise et al. (2021) included. Across all plots, the BT pegmatite variety plots most similarly to the Evje-Iveland, Froland, and Tørdal NYF/DPA-2 pegmatite varieties, implying that the BT variety may belong to NYF and DPA-2 groups. It is more difficult to determine, however, to which groups the MS+T and GT+T varieties may belong based solely on these trace element plots. These two varieties most often plot amongst LCT pegmatites, but even then generally appear on the border between the denser NYF/DPA-2 cloud and the more scattered LCT cloud apparent in each plot—unhelpful for attempting to determine their Černý (1991) classification. In most cases, it is generally apparent that the GT+T variety appears closer to the NYF/DPA-2 cloud than the MS+T variety, however. Both varieties do show remarkable overlap with Oxford County and Borborema LCT/DPA-1 pegmatites in the Al-Ti, Al-Ge, Al-B, Ge/Ti-Al/Ti, and Ge/Ti-B plots, but plot most similarly to Tres Arroyos and Hagendorf LCT/RMG-1 pegmatites in the Al-Li and Ge/Ti-Li plots, suggesting that Li concentrations in quartz from the MS+T and GT+T pegmatites are most similar to that of quartz from RMG-1 pegmatites, while all other quartz trace element concentrations are instead most similar to quartz from DPA-1 pegmatites.

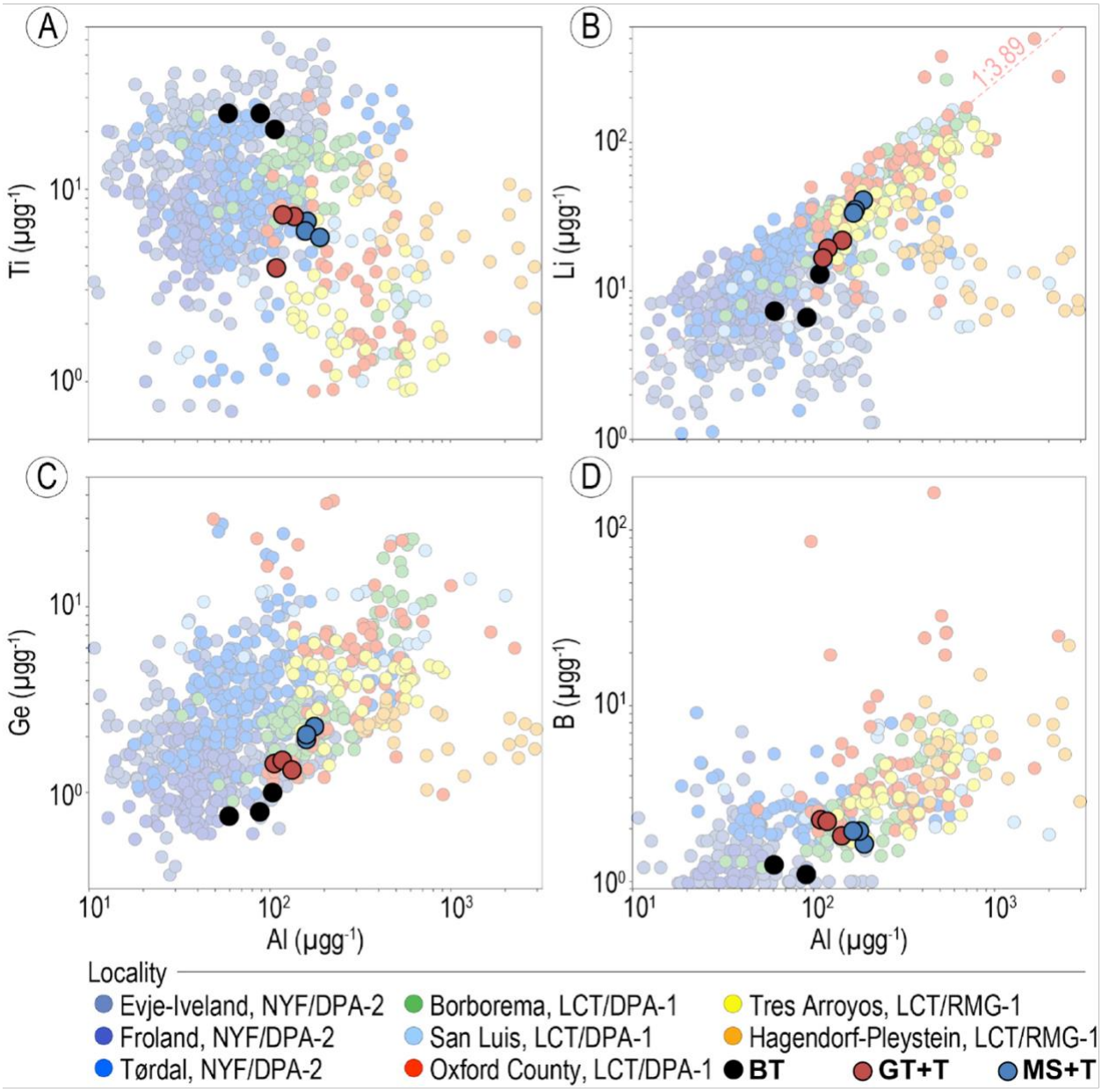

Figure 4.1 Binary trace element plots adapted from Müller et al. (2021), with quartz grains from the three Lewiston Quadrangle pegmatite varieties plotted in on field along with various other pegmatites from elsewhere in the world.

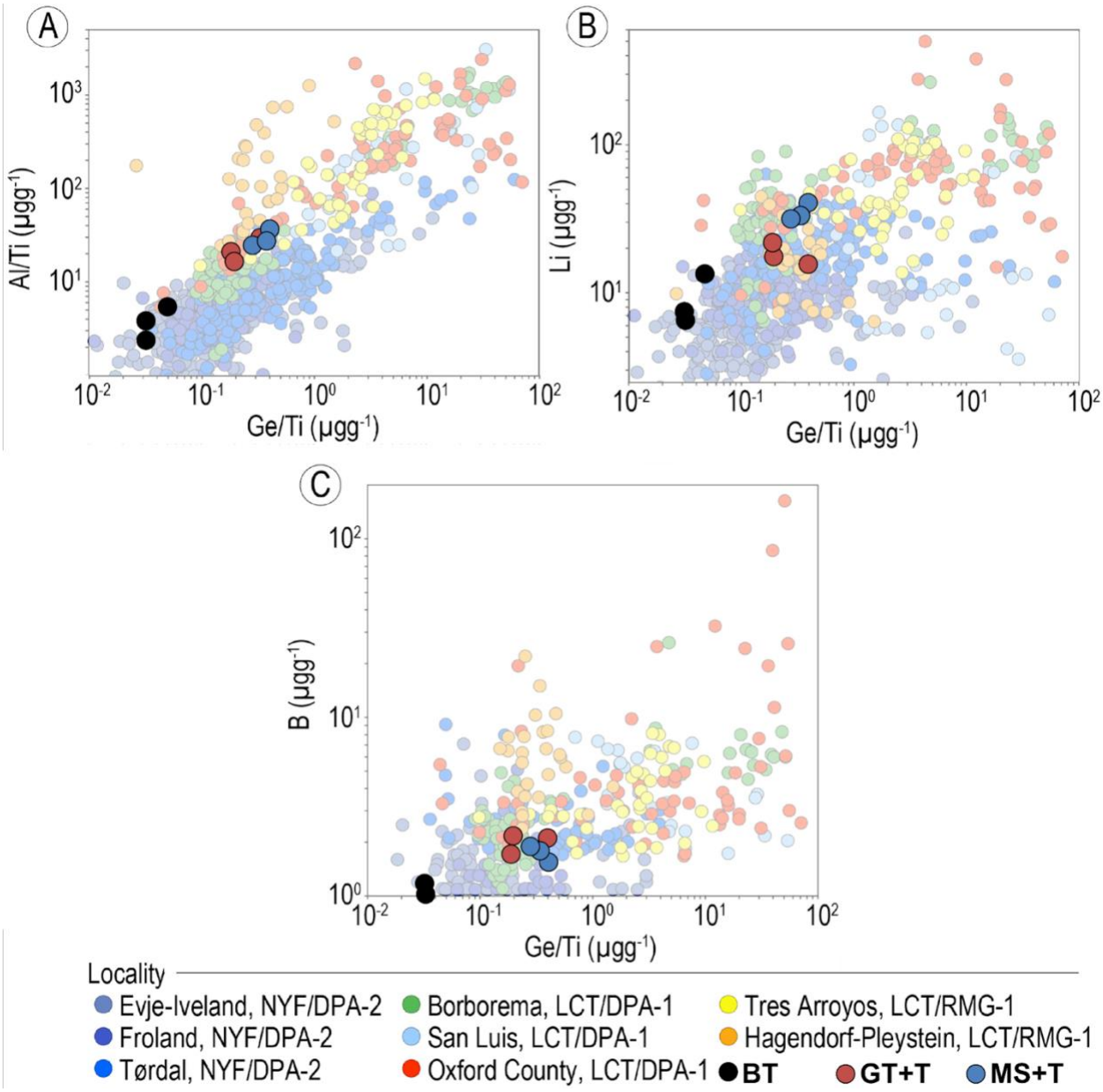

Figure 4.2 Additional plots adapted from Müller et al. (2021), this time with certain trace elements plotted against Ge/Ti instead of Al.

4.3 TitaniQ-derived Crystallization Temperatures

Ti concentrations for the nine pegmatitic quartz grains can be used to approximate the crystallization temperature of those grains through the use of the TitaniQ geothermometer (Wark

and Watson 2006), which relates Ti content of quartz in ppm $\left(X_{Ti}^{qtz}\right)$ to its crystallization temperature in degrees kelvin (T) in the following manner:

$$\log\left(X_{Ti}^{qtz}\right) = (5.69 \pm 0.02) - \frac{(3765 \pm 24)}{T}$$

Ti concentrations seen in Table 3.3 yielded an average quartz crystallization temperature of 597 °C for the BT pegmatite variety, 491 °C for the GT+T variety, and 493 °C for the MS+T variety. Quartz is traditionally the last phase to crystallize in granitic igneous rocks (Bowen 1912), so these values can be assumed to represent the final crystallization temperatures of these pegmatites as a whole. These temperatures seem to be mostly in-line with general pegmatite crystallization temperatures determined through two-feldspar thermometry (Simmons and Webber 2008), though such temperatures still seem quite varied. The crystallization temperature of the BT variety is notably about 100 °C higher than either of the other varieties at nearly 600 °C, and is therefore less similar to that of a pegmatite and more akin to that of a granite (Ackerson et al. 2018). As it was observed during sampling that the BT pegmatite variety exhibited a more granitic texture than either other variety, this difference in texture when compared to the other two pegmatites could therefore be reflective of this higher crystallization temperature. Meanwhile, the GT+T and MS+T pegmatite varieties had near-identical crystallization temperatures. Quartz grains from these two varieties have greater concentrations of the moderately incompatible elements Li, Be, B, and Ge than quartz from the BT variety, as seen in Figure 3.5 and Table 3.3, so relative enrichment in incompatible elements may be the most likely reason for the lower crystallization temperature of the two tourmaline-bearing pegmatite varieties, as an increase in incompatible elements correlates with a decrease in melt crystallization temperature (Simmons and Webber 2008).

4.4 Pegmatite Classification by Geochemical Signature

Figure 3.3 shows that the MS+T pegmatite variety is enriched in Ta, and relatively depleted in Y and REEs. It also contains the highest concentration of Li of any of the pegmatite varieties, as seen in Figure 3.5d. Although the whole rock Li content was not measured, greater Li concentration in quartz is indicative of a greater degree of Li saturation in the melt, and therefore the rock itself (Müller et al. 2021), so one may reasonably assume that the MS+T variety is also fairly enriched in Li as a whole. One might therefore move to classify the MS+T variety as being most similar to an LCT pegmatite, but its unremarkable enrichment in Cs—approximately equal to its enrichment in Nb—would make such a classification disingenuous. Considering parameters from Černý (1991), it would therefore be most apt to classify MS+T as being similar to an LCT-leaning Mixed pegmatite. The other two pegmatites are equally difficult to classify into either the NYF or LCT families by geochemical signature alone. Figure 3.3 shows that GT+T is highly enriched in certain elements indicative of an NYF classification, such as U, Th, Y, and REEs, but is relatively depleted in other elements indicative of such a classification, such as Nb and Ti (Černý 1991). However, much like the MS+T variety, GT+T is also enriched in some elements indicative of an LCT classification, such as Ta, and may be considered somewhat enriched in Cs as well, as GT+T is the only variety in which Cs is more enriched than the adjacent Rb. The GT+T variety may therefore be most similar to a Mixed pegmatite, as some patterns in its geochemical signature indicate an LCT classification, while others suggest an NYF classification. Figures 3.3 and 3.4 show that the BT pegmatite variety is highly enriched in LREEs and relatively depleted in Cs, and Figure 3.5d shows that its quartz grains contain the least Li of any pegmatite variety. However, this variety is also comparatively depleted in HREEs, and is enriched in Ta in comparison to Nb, much like the other two varieties.

Therefore, it would also be classified as being most similar to a Mixed pegmatite, as no trace element data strongly indicates that it should be classified as either NYF or LCT.

The geochemical signatures of the three Lewiston Quadrangle pegmatite varieties indicate that they could potentially fall into several of the classes defined by Černý and Ercit (2005). For instance, Figure 3.3 shows that the GT+T pegmatite is enriched in U, Th, and REEs, which implies that it could potentially fall into one of four classes: Abyssal, Muscovite–Rare-element, Rare-element, or Miarolitic (Černý and Ercit 2005). However, in all such cases, the mineral assemblages characteristic of these classes do not match that of the Lewiston Quadrangle pegmatites, which are not observed to contain any minerals except for quartz, feldspar, muscovite, biotite, garnet, and schorl (Hussey 1983). Interestingly enough, the only pegmatite class from Černý and Ercit (2005) which features a mineral assemblage similar to the Lewiston Quadrangle pegmatites is the Muscovite class, noted to contain muscovite, biotite, and almandine-spessartine garnet. However, these pegmatites are also noted to be enriched in Ba and Sr, and as all Lewiston Quadrangle pegmatites are notably depleted in these elements relative to others, they therefore cannot be considered members of the Muscovite class either. Notably, the Mt. Mica pegmatite from the Oxford County Pegmatite Field in Maine is listed as an MI-lepidolite pegmatite, which is defined by a geochemical signature enriched in Li, Be, B, and F. Whole rock concentrations for these elements were not obtained for the Lewiston Quadrangle pegmatites, but it is possible that the MS+T and GT+T varieties may have concentrations of these elements similar to those of Oxford County pegmatites such as Mt. Mica, as one may recall that their quartz grains plotted quite similarly to Oxford County pegmatite quartz grains, as seen in Figures 4.1 and 4.2. Overall, however, the Lewiston Quadrangle pegmatites seemingly defy classification according to Černý and Ercit (2005).

Using geochemical signatures to attempt classifying the Lewiston Quadrangle pegmatites according to the Wise et al. (2021) classification scheme yields slightly more conclusive results. The MS+T variety, as seen in Figure 3.3, is enriched in Rb and Ta, relatively depleted in REEs, and may be considered equally enriched in Cs and Nb. Therefore, it would most accurately fall into the RMG-1 pegmatite group, implying that it would have originated from a residual granitic melt rather than as a direct product of anatexis. While there is great precedence for LCT pegmatites derived from anatexis in Maine, such as the aforementioned Mt. Mica pegmatite in Oxford County, geochemical analysis of that pegmatite shows that it features no Eu anomaly (Simmons et al. 2016), while the MS+T variety would feature a highly negative Eu anomaly, had the detection limit for Eu been lower. This would imply that direct anatexis could perhaps be the less likely choice for this pegmatite's formation. Figure 3.3 shows that the GT+T variety is relatively depleted in Nb compared to most other trace elements, and could only therefore fall into either the DPA-2 or DPA-3 groups. Due to its obvious enrichment in U and REEs, the DPA-2 group would be the most apt classification, though its enrichment in Be as a whole is currently unknown. This would imply that the GT+T variety likely derives from anatexis of the country rock during some metamorphic event. Figure 3.4 shows that the BT variety is enriched in LREEs, but much less so in HREEs, and is otherwise only greatly enriched in Th and U according to Figure 3.3. It could therefore also be classified as a DPA-2 pegmatite, although Be concentrations are again unknown. This implies that this final pegmatite variety may be derived from anatexis of country rock as well.

4.5 Origin of Lewiston Quadrangle Pegmatites

The geochemical signature of the MS+T pegmatite variety suggests that it is most similar to a Mixed-LCT/RMG-1 pegmatite due to its enrichment in Ta and Rb, its relative depletion in

REEs, and its approximately equal enrichment in Cs and Nb. Data obtained from geochemical analysis of quartz grains seen in Figures 4.1 and 4.2 partially refutes this, however, showing that quartz from this variety is generally most similar to quartz from LCT/DPA-1 pegmatites in western Maine and northeast Brazil, but does have lithium concentrations more similar to LCT/RMG-1 pegmatites in western Spain and southeast Germany. Synthesizing whole rock and quartz grain data, the Mixed-LCT classification therefore remains accurate for this pegmatite variety, but its melt origin is still up for debate. In any case, it is known that this pegmatite derives from an enriched source, and likely crystallized at temperatures near 493 °C, but more research is still needed in order to conclude whether the melt from which this pegmatite derives was generated by anatexis, or was a residual granitic melt, as no definitive conclusion can be made based on this data. If derived from residual granitic melts, the MS+T pegmatite variety would likely be derived from one of the granite or granodiorite units mapped by Hussey (1983), as those are the only granitoid units currently known to lie within the Lewiston Quadrangle. Otherwise, it would likely be derived from anatexis of the Sangerville Formation during some metamorphic event, as the MS+T pegmatite variety is only currently known to occur within that unit. DPA-1 pegmatites are known to derive from granulite to amphibolite facies metasediments (Wise et al. 2021), and as the Sangerville Formation is known to primarily consist of sedimentary rocks which have undergone high-temperature metamorphism (Hussey 1983), this may provide additional evidence for an anatectically-derived MS+T pegmatite.

The geochemical signature of the GT+T pegmatite variety seems most similar to that of a Mixed/DPA-2 pegmatite overall, based on its enrichment in Ta, U, Y, and REEs, its moderate enrichment in Cs, and its relative depletion in Nb. However, similarly to the MS+T variety, pegmatitic quartz analysis shows that GT+T quartz is generally most similar to quartz from

LCT/DPA-1 pegmatites, but again has lithium concentrations most similar to quartz from LCT/RMG-1 pegmatites, neither of which are DPA-2 pegmatites, confusingly enough. Again synthesizing whole rock and quartz grain geochemical data, this pegmatite also has a composition most similar to a Mixed-LCT pegmatite, is derived from a depleted source melt, and likely crystallized at temperatures near 491 °C. However, similarly to the MS+T variety, it cannot be definitively determined whether this pegmatite derives from direct anatexis or a residual granitic melt, but direct anatexis is perhaps more likely in this case, given geochemical data. More research is therefore needed in order to determine the exact origins of this pegmatite as well. If this variety were truly a DPA-2 pegmatite, it should originate from direct anatexis of some granulite to amphibolite facies F-rich amphibolite, or a metaigneous rock of granitic A-type signature (Wise et al. 2021). The GT+T variety is currently only known to occur within the Patch Mountain subunit of the Sangerville Formation, which is neither an amphibolite nor a metaigneous rock, providing some evidence refuting an anatectically-derived GT+T pegmatite. However, this is based on a sample size of only two pegmatite outcrops, so it may not be accurate to say that the GT+T pegmatite must be derived from that subunit if it is derived from anatexis, as modern mapping efforts are still underway. As the GT+T variety did display similarities to a DPA-1 or RMG-1 pegmatite in the binary trace element plots seen in Figures 4.1 and 4.2, it is also possible that it may derive from one of the units listed as a potential source for the MS+T variety. The formation of the MS+T variety may have left that source depleted in LREEs, allowing the formation of the similarly LREE-depleted GT+T pegmatite in its wake. Even if that were the case, and the MS+T and GT+T varieties are derived from the same source, they cannot in good faith be considered the exact same pegmatite variety, due to obvious differences in their geochemical signatures, and the enrichments of their sources.

The BT pegmatite variety may have the most conclusive origin story of the three pegmatite varieties which occur within the Lewiston Quadrangle. Binary trace element plots for quartz grains from this variety seen in Figures 4.1 and 4.2 differentiate it from the other two varieties, as it consistently plots among NYF/DPA-2 pegmatites. However, whole rock trace element and REE data seen in Figures 3.3 and 3.4 show that this variety is not greatly enriched in Nb or Y, nor is it notably enriched in Cs or Ta, and while it is greatly enriched in LREEs, it is comparatively depleted in HREEs. Therefore, based on whole rock geochemical data, this pegmatite is most similar to a Mixed/DPA-2 pegmatite, similarly to the GT+T variety, but may lean towards an NYF/DPA-2 classification, based on where its quartz grains tend to plot. As this variety's classification as a DPA-2 pegmatite is quite consistent, this pegmatite should have originated from direct anatexis of a granulite to amphibolite facies F-rich amphibolite, or a metaigneous rock of granitic A-type signature (Wise et al. 2021), as discussed in the case of the GT+T variety. The BT pegmatite variety is only currently known to occur within the Vassalboro Formation, a quartz-plagioclase-biotite granofels known to contain amphibole minerals such as hornblende and actinolite (Hussey 1983, West and Cubley 2010). This falls solidly within the granulite facies to amphibolite facies zone, so one may reasonably conclude that the BT pegmatite variety formed from direct anatexis of the Vassalboro Formation in association with some as of now undetermined metamorphic event. The BT pegmatite is therefore overall most similar to a Mixed-NYF/DPA-2 pegmatite, and likely formed from an enriched source melt derived from the anatexis of the Vassalboro Formation, though more evidence is needed to prove this prediction as fact. This melt would have likely crystallized at 597 °C, resulting in a pegmatite which may be considered distinctively different and more granite-like than the other two pegmatite varieties found within the Lewiston Quadrangle.

5 Conclusion

5.1 Conclusions of This Study

This study tentatively concludes that the MS+T and GT+T pegmatite varieties are both similar to LCT-leaning Mixed pegmatites, and that the BT variety is similar to an NYF-leaning Mixed pegmatite. While exact mechanisms of formation cannot be conclusively determined for the MS+T and GT+T pegmatite varieties based on this study, it is likely that they derive from either direct anatexis of one or more subunits within the Sangerville Formation during some metamorphic or orogenic event, or from residual granitic melts related to one or both of the two granitoid units found within the Lewiston Quadrangle (Hussey 1983), subsequently crystallizing at similar temperatures. Due to a few similarities between these two varieties, it is theorized that they may derived from the same source. If this is so, it is possible that the formation of the MS+T variety caused that source to become depleted in LREEs, allowing for the formation of the geochemically-distinct GT+T variety. The BT+T variety most likely derives from anatexis of the Vassalboro Formation during some currently-undetermined metamorphic event, and crystallized at a higher temperature than either other pegmatite variety, resulting in the more granite-like texture seen in the field. In any case, geochemical evidence shows that the MS+T, GT+T, and BT pegmatite varieties found throughout the Lewiston 15-minute Quadrangle must be considered entirely different pegmatite varieties, due to obvious differences in crystallization temperature, source enrichment, rare element concentrations, and potential source rocks.

5.2 Future Studies

As it is still currently unknown whether the MS+T and GT+T varieties derive from anatexis or residual granitic melts, future research opportunities may involve the comparison of these pegmatites' geochemical signatures with those of local rock units both granitoid and metasedimentary, comparing them in order to hopefully determine more accurately from what

rock unit these pegmatites may be derived. One may also attempt to determine the granitic type of nearby granitoids, and whether they are peraluminous or not. If they are peraluminous and S-type, this may provide additional support for a residual granitic melt-derived origin for the MS+T and/or GT+T pegmatite varieties, as RMG-1 pegmatites are derived from peraluminous, S-type granitic melts (Wise et al. 2021). Dating these pegmatites and comparing their ages with those of nearby granitoid bodies may also provide evidence for or against a residual granitic melt-derived origin for these pegmatites, as a pegmatite and the granite from which it derives should reasonably have similar ages (Nie et al. 2020). Comparing their ages with those of metamorphic events that are known to have affected this region may provide evidence for or against an anatectic origin. It would also be prudent to determine whole rock Li, Be, B, and F concentrations for these pegmatites, as they share some similarities with MI-lepidolite Oxford County, Maine pegmatites, and may therefore be overall enriched in these elements, allowing one to potentially classify them both as a MI-lepidolite pegmatites as well (Černý and Ercit 2005), and implying that miarolitic cavities may exist somewhere within these pegmatites, and have yet to be located. Li and F concentrations may also be helpful for more accurately determining these pegmatites' classifications according to the Černý (1991) classification scheme, while Be concentrations may assist in more accurately determining these pegmatites' classifications according to the Wise et al. (2021) scheme. Notably, quartz from the MS+T pegmatite was found to contain >30 ppm Li and >100 ppm Al, as seen in Figures 3.5a and 3.5d, indicative of economic spodumene or montebrasite mineralization (Müller et al. 2021), though neither of these minerals are currently known to occur within that variety. One might therefore attempt to find solid physical evidence of the lithium ore mineralization implied by the MS+T variety's Li and Al concentrations, as such minerals may be of economic interest.

Potential future research involving the BT pegmatite variety could involve determining whether this variety and the lithologically-similar Bowdoinham Quadrangle "Biotite granite and pegmatite" unit are one and the same. This would provide further support for the theory that this pegmatite variety formed from anatexis of the Vassalboro Formation, as the "Biotite granite and pegmatite" unit is only known to occur within the Vassalboro Formation in the Bowdoinham Quadrangle (West and Cubley 2010). Dating this pegmatite to determine its age may be prudent as well, as its age may correspond with those of metamorphic events which this region is known to have been affected by. This pegmatite may also be considered one of the chemically-primitive NYF/DPA-2 pegmatites described by Müller et al. (2021), due to high concentrations of Ti and low concentrations of Ge and Li in quartz, as seen in Figures 3.5b-d. If this is truly the case, the quartz contained therein may perhaps contain low-enough rare element concentrations to be considered suitable for "high-tech application", and would therefore be of economic interest.

References

Ackerson, M.R., Mysen, B.O., Tailby, N.D., and Watson, E.B. (2018) Low-temperature crystallization of granites and the implications for crustal magmatism. Nature, 559, 94-97.

Bowen, N.L. (1912) The order of crystallization in igneous rocks. The Journal of Geology, 20, 457-468.

Bradley, D., Shea, E., Buchwaldt, R., Bowring, S., Benowitz, J., O'Sullivan, P., and McCauley, A. (2016) Geochronology and Tectonic Context of Lithium-cesium-tantalum Pegmatites in the Appalachians. The Canadian Mineralogist, 54, 945-969.

Černý, P. (1991) Rare-element granitic pegmatites. Part 1: Anatomy and internal evolution of pegmatite deposits. Part 2: Regional to global environments and petrogenesis. Geoscience Canada, 18, 49-81.

Černý, P., and Ercit, T.S. (2005) The classification of granitic pegmatites revisited. The Canadian Mineralogist, 43, 2005-2026.

Hussey, A.M. II (1983) Bedrock geology of the Lewiston 15-minute Quadrangle, Maine. Maine Geological Survey, Open-File No. 83-4. Maine Geological Survey Maps, 321.

Fedele, L., Lustrino, M., Melluso, L., Morra, V., Zanetti, A., Vannucci, R. (2015) Trace-element partitioning between plagioclase, alkali feldspar, Ti-magnetite, biotite, apatite, and evolved potassic liquids from Campi Flegrei (Southern Italy). American Mineralogist, 100, 233-249.

Marvinney, R. G. (2012) Bedrock Geology of Maine. Maine Geological Survey Fact Sheets (Online) (accessed March 28, 2022).

Mbowou, G.I.B., Botelho, N.F., Lagmet, C.A., and Ngounouno, I. (2015) Petrology of peraluminous and peralkaline rhyolites from the SE Lake Chad (northernmost Cameroon Line). Journal of African Earth Sciences, 112, 129-141.

McDonough, W.F., and Sun, W. (1995) The Composition of the Earth. Chemical Geology, 120, 223-253.

Miliszkiewicz, N., Walas, S., and Tobiasz, A., (2015) Current approaches to calibration of LA-ICP-MS analysis. Journal of Analytical Atomic Spectrometry, 30, 327-338.

Miller, C.F., and Mittlefehldt, D.W. (1982) Depletion of light rare-earth elements in felsic magmas. Geology, 10, 129-133.

Müller, A., Keyser, W., Simmons, W.B., Webber, K., Wise, M., Beurlen, H., Garate-Olave, I., Roda-Robles, E., and Galliski, M.A. (2021) Quartz chemistry of granitic pegmatites: Implications for classification, genesis and exploration. Chemical Geology, 54.

Nie, X., Wang, Z., Chen, L., Wang, G., and Li, Z. (2020) Geochemical contrasts between late triassic Rb-rich and barren pegmatites from Ningshan Pegmatite District, South Qinling Orogen, China: Implications for petrogenesis and rare metal exploration. Minerals, 10, 582.

Osberg, P.H. (1988) Geologic relations within the shale-wacke sequence in south-central Maine. Maine Geological Survey, Studies in Maine Geology, 1, 51-73. Maine Geological Survey Publications, 54.

Osberg, P.H., Hussey, A.M. II, and Boone, G.M. (1985) Bedrock geologic map of Maine. Maine Geological Survey, Maine Geological Survey Maps, 23.

Paton, C., Hellstrom, J., Paul, B., Woodhead, J., and Hergt, J. (2011) Iolite: Freeware for the visualisation and processing of mass spectrometric data. Journal of Analytical Atomic Spectrometry, 26, 2508-2518.

Rahabi, Z. (2021) Mount David, Lewiston, Maine. Maine Geological Survey, Geologic Facts and Localities, Circular GFL-257. Maine Geological Survey Publications, 613.

Robinson, P., Tucker, R.D., Bradley, D., Berry, H.N., IV, and Osberg, P.H. (1998) Paleozoic orogens in New England. GFF, 120, 119-148.

Rollinson, H., and Pease, V. (2021) Using Major Element Data. In Using Geochemical Data: To Understand Geological Processes, p. 49-95. Cambridge University Press, U.K.

Sharma, I. (2020) ICP-OES: An advance tool in biological research. Open Journal of Environmental Biology, 5, 27-33.

Simmons, W., Falster, A., Webber, K., Roda-Robles, E., Boudreaux, A.P., Grassi, L.R., and Freeman, G. (2016) Bulk composition of Mt. Mica pegmatite, Maine, USA: Implications for the origin of an LCT type pegmatite by anatexis. The Canadian Mineralogist, 54, 1053-1070.

Simmons, W.B., and Webber, K.L. (2008) Pegmatite genesis: state of the art. European Journal of Mineralogy, 20, 421-438.

Stemprok, M. (1989) Pegmatitic ore deposits. In D.R. Bowes, Ed., The Encyclopedia of Igneous and Metamorphic Petrology. Springer, Boston, Massachusetts.

Tyler, G. (1995) ICP-OES, ICP-MS and AAS Techniques Compared. ICP Optical Emission Spectroscopy Technical Notes, 05.

Wark, D.A., and Watson, E.B. (2006) TitaniQ: a titanium-in-quartz geothermometer. Contributions to Mineralogy and Petrology, 152, 743-754.

Webber, K., Falster, A.U., Simmons, W.B., and Hanson, S. (2019) Anatectic pegmatites of the Oxford County Pegmatite Field, Maine, USA. The Canadian Mineralogist, 57, 811-815.

West, D.P. Jr., and Cubley, J.F. (2010) Bedrock geology of the Bowdoinham 7.5' Quadrangle, Maine. Maine Geological Survey, Open-File Map 10-20. Maine Geological Survey Maps, 46.

White, W.M. (2013) Geochemistry, 668 p. Wiley-Blackwell, Hoboken, New Jersey.

Wilschefski, S.C., and Baxter, M.R. (2019) Inductively Coupled Plasma Mass Spectrometry: Introduction to Analytical Aspects. The Clinical Biochemist Reviews, 40, 115-133.

Wise, M.A., Müller, A., Simmons, W.B. (2021) A proposed new mineralogical classification system for granitic pegmatites. The Canadian Mineralogist, 56, 1-25.

Woodhead, J., Hellstrom, J., Hergt, J., Greig, A., and Maas, R. (2007) Isotopic and elemental imaging of geological materials by laser ablation Inductively Coupled Plasma mass spectrometry. Journal of Geostandards and Geoanalytical Research, 31, 331-343.

Appendix: Glossary of Abbreviations, Acronyms, and Symbols

AB	Abyssal
Ag	Silver
Al	Aluminum
Al_2O_3	Aluminum oxide
As	Arsenic
A/CNK	Aluminum oxide over calcium, sodium, and potassium oxides
A/NK	Aluminum oxide over sodium and potassium oxides
B	Boron
Ba	Barium
Be	Beryllium
Bi	Bismuth
BT	Biotite
cm	Centimeter
CaO	Calcium oxide
CI	Carbonaceous Ivuna
Ce	Cerium
Co	Cobalt
Cr	Chromium
Cs	Cesium
Cu	Copper
DPA	Direct products of anatexis
DRS	Data reduction scheme

Dy	Dysprosium
Er	Erbium
Eu	Europium
F	Fluorine
Fe_2O_3	Iron (III) oxide
Ga	Gallium
Ge	Germanium
Gd	Gadolinium
GT+T	Garnet + Tourmaline
Hf	Hafnium
Ho	Holmium
HREE	Heavy rare earth elements
Hz	Hertz
ICP-MS	Inductively coupled plasma mass spectrometry
ICP-OES	Inductively coupled plasma optical emission spectrometry
In	Indium
J	Joules
K	Potassium
K_2O	Potassium oxide
La	Lanthanum
LA-ICP-MS	Laser ablation inductively coupled plasma mass spectrometry
LCT	Lithium-cesium-tantalum
Li	Lithium

LOI	Loss on ignition
LREE	Light rare earth elements
Lu	Lutetium
MgO	Magnesium oxide
MI	Miarolitic
mm	Millimeter
MnO	Manganese oxide
Mo	Molybdenum
MS	Muscovite
MS+T	Muscovite + Tourmaline
MSREL	Muscovite–Rare-element
NaO	Sodium oxide
Nb	Niobium
Nd	Neodymium
Ni	Nickel
NIST	National Institute of Standards and Technology
NYF	Niobium-yttrium-fluorine
P_2O_5	Phosphorus pentoxide
Pb	Lead
peg	Pegmatite
ppb	Parts per billion
ppm	Parts per million
ppt	Parts per trillion

Pr	Praseodymium
Rb	Rubidium
REE	Rare earth elements
REL	Rare-element
RMG	Residual melts of granite magmatism
Sb	Antimony
Sc	Scandium
sec	Seconds
SiO_2	Silicon dioxide
Sm	Samarium
Sn	Tin
Sr	Strontium
T	Temperature
Ta	Tantalum
TAS	Total alkali-silica
Tb	Terbium
Th	Thorium
Ti	Titanium
TiO_2	Titanium dioxide
Tl	Thallium
Tm	Thulium
U	Uranium
V	Vanadium

W	Tungsten
wt%	Weight percent
X_{Ti}^{qtz}	Ti content of quartz in ppm
Y	Yttrium
Yb	Ytterbium
Zn	Zinc
Zr	Zircon
^{28}Si	Silicon-28
$\mu g g^{-1}$	Micrograms per gram
µm	Micrometer
%	Percent
°C	Degrees celsius
<	Less than
>	Greater than